Heliyon 9 (2023) e17801

Contents lists available at ScienceDirect

Heliyon

journal homepage: www.cell.com/heliyon

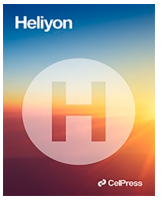

# Biological activities of 4H-thiochromen-4-one 1,1-dioxide derivatives against tropical disease parasites: A target-based drug design approach

Cristian Ortiz [a], Matthias Breuning [b], Sara Robledo [c], Fernando Echeverri [a], Esteban Vargas [a,**], Wiston Quiñones [a,*]

[a] Facultad de Ciencias Exactas Y Naturales, Universidad de Antioquia, Colombia
[b] Fakultät für Biologie, Chemie und Geowissenschaften, Universität Bayreuth, Germany
[c] Facultad de Medicina, Universidad de Antioquia, Colombia

ARTICLE INFO

*Keywords:*
Tropical diseases
Reactive oxygen species
Trypanothione reductase
Bioisosteric replacements
Allosteric inhibition

ABSTRACT

A promising strategy for developing novel therapies against tropical diseases, including malaria, leishmaniasis, and trypanosomiasis, is to detect biological targets such as trypanothione reductase, a vital parasite enzyme that regulates oxidative stress. This enzyme is highly selective and conserved in the Trypanosotidae family and has an ortholog in the Plasmodium genus. Previous studies have established that an isosteric replacement of naphthoquinone's carbonyl group with a sulfone group leads to compounds with high bioactivity and selectivity (half-maximal inhibitory concentration = 3 μM against intracellular amastigotes of *L. panamensis*, selectivity index = 153 over monocytes U-937). In this study, we analyzed the reactive oxygen species (ROS) levels of parasites through indirect measurements of the tryparedoxin system after treatment with these isosteric compounds. This strategy proved that a significant increase in the ROS levels and strong mitochondrial perturbation led to the death of parasites due to cell homeostatic imbalance, confirming the compounds' effectiveness in disrupting this important metabolic pathway. To improve understanding of the parasite-molecule interaction, 27 new compounds were synthesized and assessed against parasites of the three principal tropical diseases (malaria, leishmaniasis, and trypanosomiasis), displaying an $EC_{50}$ below 10 μM and good correlation with in-silico studies, indicating that the 4H-thiochromen-4-one 1,1-dioxide core is a special allosteric modulator. It can interact in the binding pocket through key amino acids like Ser-14, Leu-17, Trp-21, Ser-109, Tyr-110, and Met-113, leading to interhelical disruption.

## 1. Introduction

According to the World Health Organization (WHO), neglected tropical diseases (NTDs) comprise 17 pathologies affecting >1 billion people worldwide. Leishmaniasis is an NTD that affects 1 million people globally, with 300,000 new cases reported each year and 20,000 deaths reported in the past 5 years. Moreover, Chagas disease affects 8 million people globally, with 10,000 deaths

* Corresponding author.
** Corresponding author.
*E-mail addresses:* esteban.vargasc@udea.edu.co (E. Vargas), wiston.quinones@udea.edu.co (W. Quiñones).

https://doi.org/10.1016/j.heliyon.2023.e17801
Received 5 March 2023; Received in revised form 12 June 2023; Accepted 28 June 2023
Available online 1 July 2023

associated with the complications caused by this disease [1] (see Schemes 1–5)

In contrast, malaria is a parasitic infection that can be caused by five species belonging to the genus *Plasmodium* and is exclusively transmitted through the bite of female Anopheles mosquitoes. Among these parasites, *P. falciparum* is considered the most prevalent, and according to WHO, approximately 200 million cases were reported in 2020 worldwide.

The disadvantages of available treatments include their several side effects, mechanism of resistance, and high cost [2]. Therefore, the development of novel therapeutic alternatives is an urgent requirement.

Several drugs, such as melarsoprol and tryparsamide, as well as pentavalent antimony salts are known to target essential pathways in trypanosomatids, e.g., thiol redox metabolism that induces oxidative stress [3]. Previous studies have evaluated the allosteric inhibitors of trypanothione reductase (TR) to identify pharmacologically active compounds that disrupt the homeostatic balance in the intracellular forms of the parasite. Studies have indicated that quinones and furans are the key compounds that can inhibit the glutathione peroxidase system as they usually exhibit high affinity toward the enzymes of the system, particularly TR [4]. Moreover, the structural analogs of quinones and naphthoquinones, including plumbagin, diospirin, lapachol, and menadione, exhibit increased antitrypanosomal activity along with high affinity toward TR. Furthermore, these compounds act as noncompetitive inhibitors of TR, causing an increase in ROS levels and their parasite unviability consequence [4,5]. The potential mechanism of action of the abovementioned compounds can be determined based on homology with their orthologs glutathione reductase (GR) enzyme that are present in other protozoa of the genus *Plasmodium falciparum*, which causes malaria [6]. Khan et al. used X-ray diffraction to demonstrate that naphthoquinone-like compounds follow a subversive mechanism that leads to the formation of the naphthoquinone–enzyme complex via covalent bonds, thus supporting the abovementioned finding [7]. Nevertheless, the expression of another type of peroxidase such as TcOYE [8] could act as a defense mechanism against molecules with suitable redox potentials, including naphthoquinones and other therapeutic alternatives from the same category of compounds.

Previous studies have demonstrated that the 4H-thiochromen-4-one 1,1-dioxide core, which is an allosteric modification of naphthoquinones, exhibits high activity and selectivity in an *in vitro* assay against intracellular amastigotes of *Leishmania* [9]. The structural modification helps the compound to escape the action of TcOYE (peroxidase enzyme). In this study, the biological activity of 27 compounds developed under allosteric site requirements that satisfied the TR and GR requirements was examined against parasites trypanosomatids and *Plasmodium*.

## 2. Material and methods

### 2.1. Electrochemical measurements

The agreement among three electrode measurements was used to assess the electrochemical behavior of the 4H-thiochromen-4-one 1,1-dioxide core. Glassy carbon was used as a working electrode, AgCl/Ag electrode was used as a reference electrode, and platinum was selected as a counter electrode. TBAB was used as a supporting electrolyte at a concentration of 0.1 M, and acetonitrile (ACN) was

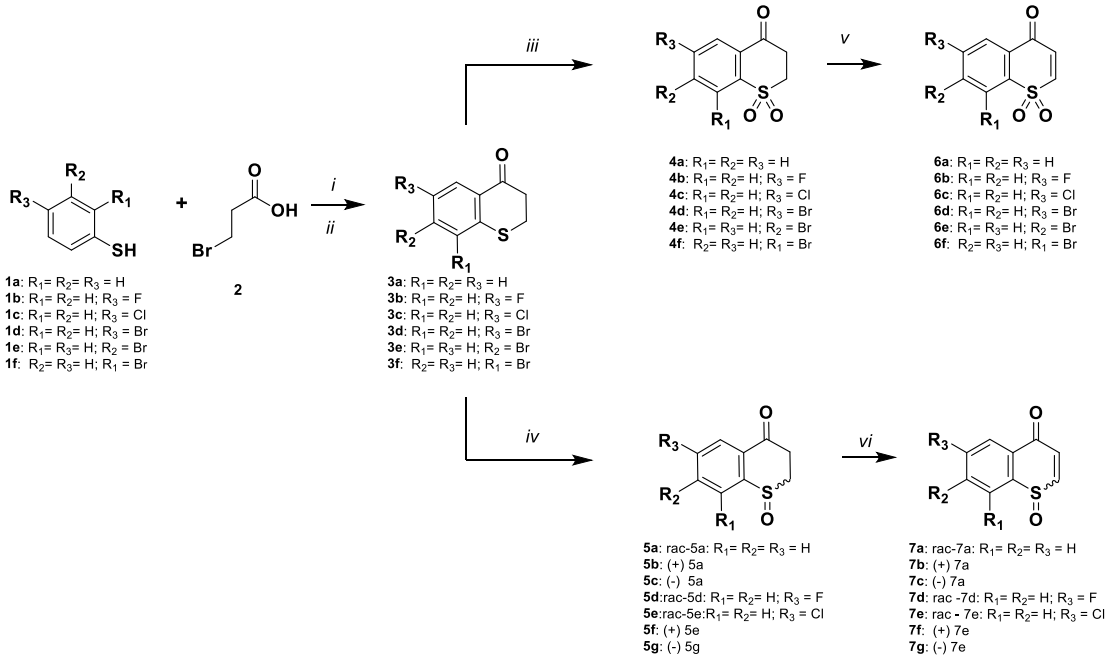


**Scheme 1.** Synthesis of the first set of derivatives: 6a–f and 7a–g. (i) $K_2CO_3/KHCO_3$; (ii) $H_2SO_4$, 0 °C; (iii) Oxone®, acetone; (iv) $Ti(OiPr)_4$, binaphthol $CCl_4$; (v) $I_2$ in DMSO, 100 °C; and (vi) DDQ, MsOH, MW irradiation.

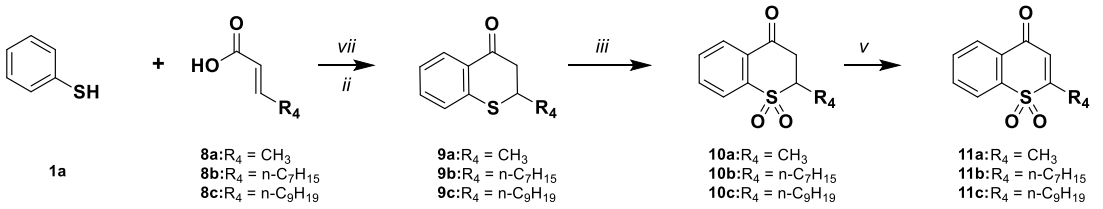


**Scheme 2.** Synthesis of the second set of derivatives: 11a–c. (vii) TBAF, $Et_3N$, ACN; (ii) $H_2SO_4$, 0 °C; (iii) Oxone®, acetone; (vi) DDQ, MsOH, MW irradiation.

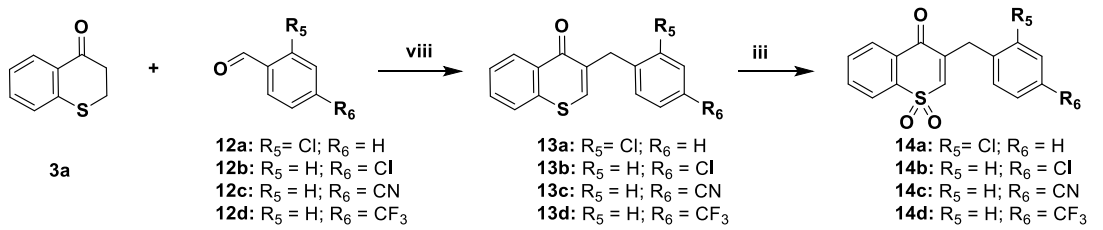


**Scheme 3.** Synthesis of the third set of derivatives: **14**a–d. (viii) Piperidine, LiBr, MW irradiation, 100 °C, (iii) Oxone ®, acetone.

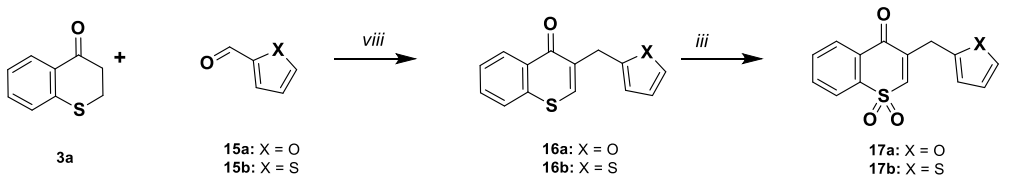


**Scheme 4.** Synthesis of the fourth set of derivatives: **17a–b.** (viii) Piperidine, LiBr, MW irradiation, 100 °C; (iii) Oxone ®, acetone.

used as the solvent. Measurements were performed using the autolab PGSTAT302 N instrument in which a scan was performed with a large potential window ranging from −1.5 to 2.5 V at a rate of 150 mV/s.

### 2.2. Reactive oxygen species measurement

The generation of reactive oxygen species (ROS) inside the amastigotes of *Leishmania braziliensis* via mechanical action was monitored using 2′7′dihydrofluorescein ($H_2$DCF-DA) as a fluorescent probe. The cell concentration of the parasites was adjusted to $1 \times 10^7$ cells/mL in M199 or RPMI-1640 medium without phenol red at pH 5.5 supplemented with 10% fetal bovine serum (FBS). After washing the cells via centrifugation with phosphate-buffered saline (PBS), they were resuspended in 100 μL of $H_2$DCF-DA probe (0.2 μg/mL Hanks's solution) and seeded into 96-well dark microplates, which were incubated for 1 h at 32 °C under protection from light. Then, dichlorofluorescein, which was derived from the oxidation of $H_2$DCFDA, was quantified based on ROS levels using a flow cytometer (LSR Fortesa, BD Biosciences, USA) [10].

### 2.3. Docking studies

Simulation of the primary interaction between the compound and target receptor was performed based on docking studies. The X-ray structure of TR in its reduced form, which was downloaded from the PDB website label 4ADW [11]. A standard procedure was followed; The molecules that do not have protein characters (such as water and ions) were deleted. Followed by polar hydrogens suppression finally, the charge needed to simulate physiological conditions was added. The protein region selected to carry out the simulation was a rectangular grid box 20 × 26 × 16 Å in length, necessary to cover the allosteric modulator widely reported in the TR enzyme. It is fixed around the catalytic amino acids.) The ligands (twenty third new compounds, and also four known molecules as positive control label as **R1**-**R4**, and **R5** like negative control) was prepared as follows. Minimization was performed using density functional theory considering the B3LYP functional and 6–31+g(d,p) as the basis according to the literature [12]. This approach was selected to obtain more accurate results than those obtained by other available options, and optimization was performed according to the VSP theory. The structure obtained in this procedure is an appropriate starting point because according to the methodology, it represents the minimum of the potential energy surface (PES) of the molecule.

To better understand the biological activity and continually improve the generation of new compounds, after the formation of the

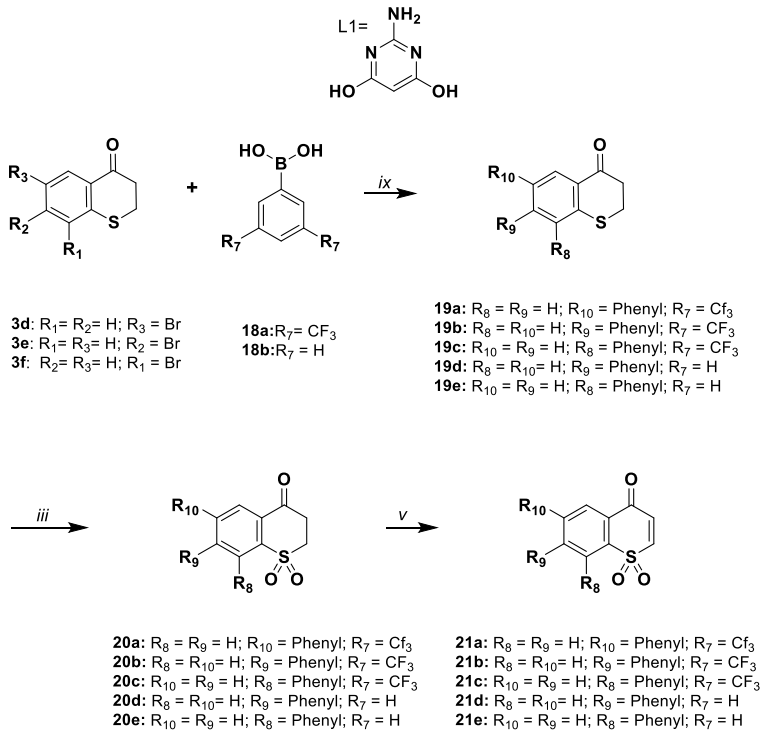


**Scheme 5.** Synthesis of the fifth set of derivatives: 21a–e. (ix) DME/$H_2O$, $Et_3N$, Pd(dppf)$Cl_2$; (iii) Oxone ®, acetone; (v): $I_2$ in DMSO, 100 °C.

two structures (the ligand and protein) was used to run two different simulation. Autodock vina algorithm [13,14] And Swiss dock algorithm [15,16] Simulation was performed using two different algorithms: Lamarckian and e CHARMM (Chemistry at Harvard Macromolecular Mechanics) algorithms implemented by Autodock and Swiss dock respectively. Thus, a score of the optimal interaction associated with the fitted position was obtained as bond energy.

### 2.4. Cytotoxic activity

Cytotoxicity of the compounds was assessed using exponential phase human monocytes (U-937 ATCC CRL-1593.2) at a concentration of $1 \times 10^5$ cells/mL in RPMI-1640 supplemented with 10% FBS. Cell suspension (100 μL) was dispensed in each well of a 96-well microplate, followed by the addition of 100 μL of each compound at various concentrations (200, 50, 12.5, and 3.125 μg/mL) or of the standard drugs (amphotericin B, chloroquine, and benznidazole) dissolved in PBS with 0.5% dimethyl sulfoxide (DMSO). Cells exposed to compounds or standard drugs were incubated for 72 h at 37 °C under 5% $CO_2$. Cytotoxic activity of each compound was defined based on the effect on the cell viability, as determined using the MTT assay in which 3-(4,5-dimethylthiazol-2-yl)-2,5-diphenyltetrazolium bromide is reduced to a purple formazan product by mitochondrial enzyme succinate dehydrogenase. For this assay, 10 μL of MTT solution (5 mg/mL) was added to each well of treated and control cells, and plates were incubated at 37 °C under 5% $CO_2$ for 3 h. The reaction was stopped by adding 100 μL of 50% isopropanol and 10% sodium dodecyl sulfate per well. Formazan levels were determined spectrophotometrically at 570 nm (Varioskan, Thermo, Waltham, MA, USA), and color intensity (absorbance) was acquired as the optical density (O.D.). Cells incubated with the standard drugs were used as toxicity controls (positive control), whereas those incubated in the absence of any compound were used as viability controls (negative control). Nonspecific absorbance was corrected by subtracting the absorbance (O.D) of the blank samples from the measured value. Experiments were performed in triplicates of at least two independent experiments [17].

### 2.5. Antileishmanial activity

The antileishmanial activity of compounds was determined based on the efficacy of the compounds in reducing infections caused by *L. panamensis*. To this end, the antileishmanial activity of the compounds was evaluated on the intracellular amastigotes of *L. panamensis* transfected with the green fluorescent protein gene (MHOM/CO/87/UA140-EGFP strain) [18]. Briefly, U-937 human cells at a concentration of $3 \times 10^5$ cells/mL in RPMI-1640 medium and 0.1 μg/mL of phorbol-12-myristate-13-acetate (PMA) were seeded into a 24-well microplate and then infected with stationary phase *L. panamensis* promastigotes in a parasite to cell ratio of 15:1. The plates were incubated at 34 °C under 5% $CO_2$ for 3 h; next, the cells were washed twice with PBS to eliminate noninternalized parasites. Overall, 1 mL of fresh RPMI-1640 medium was added to each well, and the plates were incubated again. After 24 h of

infection, the RPMI-1640 medium was replenished with fresh culture medium containing the tested compounds at four serial dilutions (50, 12.5, 3.125, and 0.78 μg/mL), and the plates were incubated for 72 h at 37 °C under 5% $CO_2$. Subsequently, the cells were removed from the bottom of the plate using 100 μL of EDTA/trypsin (250 mg) solution. Cells were centrifuged at 1100 rpm for 10 min at 4 °C, and the supernatant was discarded. Next, the cells were washed with 1 mL of cold PBS and centrifuged at 1100 rpm for 10 min at 4 °C. As described above, the cells were washed twice with PBS, and after the last wash, the supernatant was discarded and cells were suspended in 500 μL of PBS.

Cells were analyzed using a flow cytometer (Cytomics FC 500MPL) equipped with an argon laser at 488 (exciting) and 525 nm (emitting), and a total of 10,000 events were recorded. Infected cells were identified based on the green fluorescence events (parasites). All analyses were performed in triplicates of two experiments. Infected cells treated with the control drug (amphotericin B) were used as antileishmanial activity controls (positive control), whereas infected cells incubated in the absence of any compound or drug were used as infection controls (negative control). Nonspecific fluorescence was corrected by subtracting the fluorescence intensity of unstained cells from the measured intensity. Analyses were performed in triplicates of at least two independent experiments [19].

### 2.6. Antitrypanosomal activity

The metacyclic trypomastigotes of *Trypanosoma cruzi* (Tulahuen strain transfected with the β-galactosidase gene) were cultured at 26 °C for 10 days in modified Novy–McNeal–Nicolle medium. U-937 cells were seeded into 96-well plates at a concentration of $2.5 \times 10^4$ cells/mL, followed by the addition of 100 μL of medium and PMA, as described previously. After transformation to macrophages, the cells were infected with a parasite to cell ratio of 5:1 and incubated in RPMI-1640 medium supplemented with 10% FBS for 24 h at 37 °C under 5% $CO_2$. The cells were washed twice with PBS to remove noninternalized parasites, and fresh medium containing six serial dilutions of each testing compound or benznidazole was added. After incubating the cells for 72 h under the same conditions, the viability of intracellular amastigotes was determined by measuring the β-galactosidase activity. For this purpose, chlorophenol red-β-D-galactopyranoside (100 μM) and 0.1% Nonidet P-40 were added to each well and incubated for 4 h at 37 °C and 24 °C under protection from light.

The β-galactosidase activity was then measured at 570 nm using a Varioskan, Thermo spectrophotometer. Nonspecific absorbance was corrected by subtracting the absorbance of the blank samples from the measured value. Infected cells exposed to benznidazole (50, 12.5, and 3.125 μM) were used as antitrypanosomal activity controls (positive control), whereas nontreated cells were used as infection controls (negative control). Analyses were performed in triplicates of at least two independent experiments [19].

### 2.7. Antiplasmodial activity

The antiplasmodial activity of the compounds was evaluated *in vitro* in asynchronous cultures of *P. falciparum* (3D7 strain), which were maintained under standard culture conditions [20]. The activity of each compound was assessed by measuring the activity of lactate dehydrogenase (LDH) released from the cytosol of damaged cells into the supernatant, as previously described [20] *P. falciparum* cultures were adjusted to 0.5% parasitemia and 1% hematocrit in RPMI-1640 medium enriched with 1% Albumax II. Further, 100 μL of parasite suspension was dispensed into each well and then incubated with 100 μL of four serial dilutions of the tested compounds (100, 25, 3.125, and 0.78 μM). Infected cells exposed to chloroquine (CQ) were used as antiplasmodial activity controls (positive control), whereas nontreated cells were used as growth and viability controls (negative control). Plates were incubated for 72 h at 37 °C under $N_2$ (90%), $CO_2$ (5%), and $O_2$ (5%) atmosphere. After incubation, the plates were collected, and the cells were subjected to three cycles of freeze–thaw for 20 min. Next, 100 μL of Malstat reagent (400 μL of Triton X-100 in 80 mL of deionized water, 4 g of L-lactate, 1.32 g of Tris buffer, and 0.022 g of acetylpyridine adenine dinucleotide in 200 mL of deionized water; pH 9.0) and 25 μL of NBT/PES solution (16 g/L nitroblue tetrazolium salt and 0.8 g/L phenazine methosulfate) were added to each well of a second flat-bottom 96-well plate. The cells in each well were lysed via five cycles of freeze–thaw, lysate was homogenized by pipetting, and 15 μL of culture from each well was transferred into a replica plate containing Malstat and NBT/PES solution. After incubating for 1 h in the dark, color development of the LDH reaction was measured at 650 nm using a Varioskan, Thermo spectrofluorometer. Nonspecific absorbance was corrected by subtracting the blank value from the measured value.

### 2.8. Statistical analyses

Cytotoxicity was determined based on the viability and mortality percentages obtained for each experimental condition (synthetized compounds, amphotericin B, and culture medium). Results are expressed as the mean lethal concentrations ($LC_{50}$) that correspond to concentrations required to kill 50% of cells. $LC_{50}$ is calculated using the parametric method of linear regression that allows dose–response analysis (probit analysis) Viability percentages were initially calculated using Equation (1), where the O.D. of the control wells indicates 100% viability.

$$\%\ viability = \frac{O.D.\ exposed\ cells}{O.D.\ unexposed\ cells} \times 100 \quad (1)$$

The percentage of cell growth inhibition was then calculated using Equation (2):

$$\%\ inhibition = 100 - (\%\ Viability) \quad (2)$$

Toxicity was defined using $LC_{50}$ values based on the following scale: toxic, $LC_{50} < 100$ μM; moderately toxic, 100 μM $< LC_{50} <$ 200

μM; and potentially nontoxic, $LC_{50} > 200$ μM.

Antileishmanial activity was defined based on the reduction in percentage of fluorescent parasites determined using the median fluorescence intensity values, which were obtained for each experimental condition via flow cytometry. The parasite values for each concentration of compounds were calculated using Equation (3), where the % of parasites in the control well indicates 100% of parasites.

$$\%\ parasites = \frac{MFI\ of\ exposed\ parasites}{MFI\ of\ unexposed\ parasites} \times 100 \tag{3}$$

Next, inhibition percentage of parasites was calculated using Equation (4):

$$\%\ inhibition\ of\ parasites = 100 - (\%\ parasites) \tag{4}$$

Results of antileishmanial activities are expressed as median effective concentrations ($EC_{50}$), as determined using the probit method. The activity of each compound was determined using the $EC_{50}$ values as follows: high activity, $EC_{50} < 25$ μM; moderate activity, 25 μM $< EC_{50} <$ 100 μM; and low activity, $EC_{50} > 100$ μM.

## 2.9. Chemistry

### 2.9.1. General information

Commercially available reagents and solvents were purchased and used without further purification. Reaction progression was monitored using thin layer chromatography (TLC) on silica gel TLC aluminum sheets (Merck, $60F_{254}$). Fourier transform infrared spectroscopy (FTIR) spectra were recorded using a Bruker Alpha FTIR spectrometer (Bruker Optic GmbH). $^{1}H$ and $^{13}C$ nuclear magnetic resonance (NMR) spectra were acquired using Bruker Avance DRX300 instrument (300 MHz for $^{1}H$, 75 MHz for $^{13}C$) and Bruker Avance III HD 500 instrument (500 MHz for $^{1}H$, 125 MHz for $^{13}C$). Chemical shifts were calibrated using residual undeuterated solvent as an internal reference. High-resolution mass spectra were recorded using an ultrahigh-resolution Qq time-of-flight mass spectrometer (Impact II-Bruker) and hybrid quadrupole-Orbitrap (Thermo Fisher Scientific) with an electrospray ionization (ESI) source in the positive ion mode (reported as $[M+H]^+$ or $[M+Na]^+$).

### 2.9.2. General procedure I

**Thiochroman-4-one (3a)**

Thiophenol (2.40 g, 18.70 mmol) was dissolved in ethanol (12 mL) and a buffer solution of $K_2CO_3/KHCO_3$ (pH = 9) was then added. Following 10 min of stirring at room temperature (rt), 2-bromopropionic acid (2.90 g, 19.0 mmoL) was added, and the mixture was refluxed overnight until completion of the reaction (monitored by TLC). The aqueous layer was treated with a cold hydrochloric acid solution (20%, 20 mL) and extracted with DCM (2 × 50 mL). The combined organic layers were dried over $Na_2SO_4$. Evaporation of the solvent under reduced pressure resulted in a white solid (2.00 g, 10.97 mmol), which was cooled to 0 °C in an ice bath. Concentrated sulfuric acid (10 mL) was added, and the reaction mixture was stirred for 10 min at 0 °C, warmed to RT, and stirred for another 24 h.

The reaction mixture was quenched with ice and extracted with DCM (3 × 25 mL). The combined organic layers were washed with water (25 mL) and saturated $NaHCO_3$ solution (25 mL) and were dried over $Na_2SO_4$; further, they were concentrated under reduced pressure. The residue was purified via silica gel column chromatography using hexane:EtOAc (9:1) as an eluent to produce the pure compound **3a** (1.74 g, 10.60 mmol) as a yellowish oil with a yield of 96%.

$^{1}H$ NMR (500 MHz, $CDCl_3$) δ 8.15 (q, $J$ = 8.0 Hz, 1H), 7.42 (m, $J$ = 4.1 Hz, 1H), 7.32 (d, $J$ = 8.0 Hz, 1H), 7.22 (m, $J$ = 4.0 Hz, 1H), 3.28 (m, $J$ = 3.2 Hz, 2H), 3.02 (m, $J$ = 3.4 Hz, 2H). $^{13}C$ NMR (125 MHz, $CDCl_3$) δ 194.09, 171.19, 142.21, 133.31, 130.94, 129.24, 127.64, 125.06, 39.62, 26.65.

This procedure was used to synthesize compounds **3b–f**.

## 2.10. General procedure II

**Thiochroman-4-one 1,1-dioxide (4a)**

Thiochroman-4-one (67.4 mg, 0.370 mmol) and oxone (346 mg, 1.126 mmol) were dissolved in a ternary solvent system (MeOH, water, and acetone in a 1:1:1 v/v ratio), and the mixture was stirred at 60 °C for 12 h. After completion of the reaction (monitored by TLC), cold saturated brine (20 mL) was added, and the mixture was extracted with DCM (2 × 50 mL). The combined organic layers were dried over $Na_2SO_4$, and the solvent was removed under reduced pressure to produce the compound **4a** (55.35 mg, 0.282 mmol) as a whitish solid with a yield of 76%.

$^{1}H$ NMR (500 MHz, $CDCl_3$) δ 8.13 (d, $J$ = 0.6 Hz, 1H), 8.02 (d, $J$ = 7.8 Hz, 1H), 7.83 (dt, $J$ = 1.0, 7.6 Hz, 1H), 7.75 (t, $J$ = 8.0 Hz, 1H), 3.70 (d, $J$ = 6.6 Hz, 2H), 3.43 (d, $J$ = 6.7 Hz, 2H). $^{13}C$ NMR (125 MHz, $CDCl_3$) δ 190.23, 141.35, 135.00, 133.44, 130.24, 128.85, 123.67, 49.23, 36.71.

This procedure was used to synthesize compounds **4b–f**.

### 2.11. General procedure III

**(+)-Thiochroman-4-one 1-oxide (5b)**

The solutions of (*R*)-binaphthol (23.0 mg, 12.0 mol%), $CCl_4$ (3 mL), and $Ti(OiPr)_4$ (11.0 μL, 11.363 mg, 6.55 mol%) were added into a dry Schleck flask filled with argon. The mixture was stirred at 25 °C until the solution was homogenous. Water (20.0 μL, 19.940 mg, 1.8 equivalents) was added and the mixture was stirred for 1 h. Next, thiochroman-4-one **3a** (100 mg, 0.608 mmol) was added and the mixture was cooled to 0 °C for 2 h; then, *tert*-butyl hydroperoxide (70% in water, 160 μL, 1.22 mmol) was added to the mixture. Asymmetric oxidation was completed at 4 °C after 24 h, as assessed using TLC. The reaction mixture was quenched with brine (25 mL) and extracted with ethyl acetate (4 × 20 mL). The combined organic phases were dried over $MgSO_4$, filtered, and evaporated. Flash chromatography on silica gel (MTBE:ethyl acetate, 7:2) led to the development of the compound (+)-**5b** (104 mg, 0.578 mmol) as an orangish solid with a yield of 95%.

The enantiomeric excess was determined using HPLC on chiral phase (Chiracel AD-H [5 μm, 250 × 4.6 mm]; hexanes:isopropanol, 94:6; flow rate, 10 mL/min; detection at 215 nm; and total run time, 70 and 90 min).

Ee 70% ($t_R$, 50.82 [−] and 49.15 min [+]). $[\alpha]_D^{25} = +84.5°$ (c = 20 mg/mL in chloroform). $^1$H NMR (500 MHz, $CDCl_3$) δ 8.17 (d, *J* = 7.8 Hz, 1H), 7.88 (d, *J* = 7.4 Hz, 1H), 7.77 (t, *J* = 7.6 Hz, 1H), 7.67 (d, *J* = 15.2 Hz, 1H), 3.48 (m, *J* = 9.7 Hz, 1H), 2.90 (dd, *J* = 8.9, 14.7 Hz, 1H). $^{13}$C NMR (125 MHz, $CDCl_3$) δ 192.08, 145.62, 134.70, 132.22, 129.24, 129.06, 128.57, 46.78, 30.41. IR $\nu$ ($cm^{-1}$) 3059, 1680, 1569, 1026, 777. High-resolution mass spectrometry–ESI (HRMS–ESI) *m/z* for $C_9H_9O_2S$ $[M+H]^+$, calculated: 181.03178 and observed: 181.03159.

This procedure was used to synthesize compounds **5a–g.**

### 2.12. General procedure IV

**4*H*-Thiochromen-4-one 1,1-dioxide (6a)**

A solution of thiochroman-4-one 1,1-dioxide **4a** (100 mg, 0.509 mmol) in DMSO (2 mL) was added to a solution of $I_2$ in DMSO (0.1 M), and the mixture was heated at 100 °C overnight until the reaction was completed. The reaction mixture was quenched with brine (25 mL), and the organic layer was dried over $Na_2SO_4$. Evaporation of the solvent under reduced pressure and purification via silica gel column chromatography (pentane: EtOAc, 5:1) resulted in the formation of the pure compound **6a** (69.193 mg; 0.356 mmol) as a whitish solid with a yield of 70%. This protocol was followed for all compounds in this series to obtain an average yield of 65%.

$^1$H NMR (500 MHz, $CDCl_3$) δ 8.20 (1H, d, *J* = 7.2 Hz), 8.04 (1H, d, *J* = 8.1 Hz), 7.89 (1H, t, *J* = 8.0 Hz), 7.77 (1H, t, *J* = 7.7 Hz), 7.37 (1H, d, *J* = 13.0 Hz), 6.76 (1H, d, *J* = 11.7 Hz);$^{13}$C NMR (125 MHz, CDCl3) δ 176.78, 139.98, 139.49, 133.98, 132.07, 131.35, 127.52, 127.06, 122.50. IR $\nu$ ($cm^{-1}$) 3032, 2954, 1668, 1307, 1295, 1153, 1106, 77.47.

This procedure was used to synthesize compounds **6a–f**.

**6-Fluoro-4*H*-thiochromen-4-one 1,1-dioxide (6b)**

Yield 75%. $^1$H NMR (500 MHz, $CDCl_3$) δ 8.08 (dd, *J* = 4.7, 8.7 Hz, 1H), 7.86 (q, *J* = 3.8 Hz, 1H), 7.57 (m, *J* = 3.2 Hz, 1H), 7.38 (d, *J* = 11.5 Hz, 1H), 7.26 (s, 1H), 6.78 (d, *J* = 11.6 Hz, 1H), 1.56 (s, 1H), 1.25 (s, 1H). $^{13}$C NMR (125 MHz, $CDCl_3$) δ 176.87, (165.84, 163.79, 153 Hz), 140.91, 137.14, 132.08, 130.88, (126.79, 126.72, 8.77 Hz), (122.68, 122.50, 24.4 Hz), (115.45, 11.29, 24.2 Hz).

**6-Chloro-4*H*-thiochromen-4-one 1,1-dioxide (6c)**

Yield 70%. $^1$H NMR (500 MHz, $CDCl_3$) δ 8.15 (d, *J* = 2.0 Hz, 1H), 7.99 (d, *J* = 8.6 Hz, 1H), 7.84 (q, *J* = 3.5 Hz, 1H), 7.38 (d, *J* = 11.5 Hz, 1H), 7.26 (s, 1H), 6.77 (d, *J* = 11.5 Hz, 1H), 1.58 (s, 1H), 1.26 (d, *J* = 9.5 Hz, 1H), 0.04 (s, 1H). $^{13}$C NMR (125 MHz, $CDCl_3$) δ 176.85, 140.78, 140.15, 139.09, 135.06, 132.08, 129.32, 128.48, 125.29.

**6-Bromo-4*H*-thiochromen-4-one 1,1-dioxide (6d)**

Yield 65%. $^1$H NMR (300 MHz, $CDCl_3$) δ 8.35 (d, *J* = 1.9 Hz, 1H), 8.05 (q, *J* = 3.4 Hz, 1H), 7.95 (d, *J* = 8.4 Hz, 1H), 7.43 (d, *J* = 11.5 Hz, 1H), 7.31 (s, 1H), 6.81 (d, *J* = 11.5 Hz, 1H), 3.52 (m, *J* = 23.1 Hz, 1H), 2.14 (s, 1H). $^{13}$C NMR (75 MHz, $CDCl_3$) δ 176.82, 140.77, 139.56, 138.00, 132.06, 131.49, 129.16, 128.32, 125.23.

**7-Bromo-4*H*-thiochromen-4-one 1,1-dioxide (6e)**

Yield 68%. $^1$H NMR (500 MHz, $CDCl_3$) δ 8.16 (d, *J* = 1.7 Hz, 1H), 8.05 (d, *J* = 8.6 Hz, 1H), 7.89 (q, *J* = 3.4 Hz, 1H), 7.35 (d, *J* = 11.5 Hz, 1H), 7.26 (s, 1H), 6.76 (d, *J* = 11.6 Hz, 1H), 1.56 (s, 1H). $^{13}$C NMR (125 MHz, $CDCl_3$) δ 177.15, 141.95, 140.22, 136.50, 132.33, 130.67, 130.13, 126.71, 126.64.

**8-Bromo-4*H*-thiochromen-4-one 1,1-dioxide (6f)**

Yield 65%. $^{1}$H NMR (500 MHz, $CDCl_3$) δ 8.22 (d, $J$ = 8.0 Hz, 1H), 8.04 (d, $J$ = 8.1 Hz, 1H), 7.59 (t, $J$ = 7.9 Hz, 1H), 7.37 (d, $J$ = 11.67 Hz), 6.74 (d, $J$ = 11.5 Hz, 1H). $^{13}$C NMR (125 MHz, $CDCl_3$) δ 177.07, 141.33, 140.73, 139.09, 133.27, 130.57, 130.48, 128.19, 118.40.

### 2.13. General procedure V

#### (±)-4*H*-Thiochromen-4-one 1-oxide (7a)

Sulfoxide **5a** (50 mg, 0.262 mmol) and DDQ (71 mg, 0.323 mmol) were dissolved in dioxane (5 mL) in a microwave flask. MsOH (17. x μL, 0.262 mmol) was added under intense stirring, causing a rapid color change from dark red to orange, suggesting that DDQ was activated. The mixture was then degasified using $N_2$, the flask was sealed, and the reaction was heated at 140 °C under microwave irradiation for 2 h. After cooling to RT, the reaction mixture was quenched with brine (25 mL) and extracted with ethyl acetate (3 × 25 mL). The combined organic phases were concentrated under reduced pressure and dried over $MgSO_4$. The crude product was filtered using a silica gel pad (petroleum ether/ethyl acetate 1:0 → 3:1) to produce the compound **7d** (40.433 mg, 0.206 mmol) as a red solid with a yield of 81%.

$^{1}$H NMR (300 MHz, $CDCl_3$) δ 8.59 (d, $J$ = 8.0 Hz, 1H), 7.89 (d, $J$ = 10.5 Hz, 1H), 7.63 (m, $J$ = 5.2 Hz, 2H), 7.62 (d, $J$ = 4.2 Hz, 1H), 7.07 (d, $J$ = 10.4 Hz, 1H). $^{13}$C NMR (75 MHz, $CDCl_3$) δ 178.93, 163.85, 160.54, 138.15, 134.29–132.94, 129.02, 124.90, 120.62–120.30, 114.43–114.13. IR $\nu$ ($cm^{-1}$) 3059, 1680, 1569, 1026, 777.

This procedure was used to synthesize compounds **7a–g.**

#### (+)-4*H*-Thiochromen-4-one 1-oxide (7b)

Yield 60%. $[\alpha]_D^{25} = +85.5^{\circ}$ (c = 20 mg/mL in chloroform). $^{1}$H NMR (300 MHz, $CDCl_3$) δ 8.59 (d, $J$ = 7.8 Hz, 1H), 7.88 (d, $J$ = 10.5 Hz, 1H), 7.67 (d, $J$ = 1.0 Hz, 2H), 7.61 (d, $J$ = 4.2 Hz, 1H), 7.07 (d, $J$ = 10.5 Hz, 1H).

#### (−)-4*H*-Thiochromen-4-one 1-oxide (7c)

Yield 75%. $[\alpha]_D^{25} = -36.4^{\circ}$ (c = 20 mg/mL in chloroform). $^{1}$H NMR (300 MHz, $CDCl_3$) δ 8.59 (d, $J$ = 7.7 Hz, 1H), 7.89 (d, $J$ = 10.5 Hz, 1H), 7.67 (d, $J$ = 1.1 Hz, 2H), 7.62 (d, $J$ = 4.2 Hz, 1H), 7.58 (m, $J$ = 1.0 Hz, 1H), 7.08 (d, $J$ = 10.5 Hz, 1H).

#### (±)-6-Fluoro-4*H*-thiochromen-4-one 1-oxide (7d)

Yield 65%. $^{1}$H NMR (300 MHz, $CDCl_3$) δ 8.21 (q, $J$ = 4.1 Hz, 1H), 7.87 (d, $J$ = 10.4 Hz, 1H), 7.63 (dd, $J$ = 4.8, 8.8 Hz, 1H), 7.38 (m, $J$ = 3.2 Hz, 1H), 7.26 (s, 1H), 7.01 (d, $J$ = 10.4 Hz, 1H), 4.31 (m, $J$ = 9.8 Hz, 1H), 2.05 (s, 1H), 2.04 (s, 1H), 1.30 (q, $J$ = 11.3 Hz, 1H), 0.90 (q, $J$ = 6.6 Hz, 1H). $^{13}$C NMR (75 MHz, $CDCl_3$) δ 178.93, 163.85, 160.54, 138.15, 134.19, 132.94, 129.02, 128.92, 124.90, 120.62, 120.30, 114.43, 114.37.

#### (±)-6-Chloro-4*H*-thiochromen-4-one 1-oxide (7e)

Yield 85%. $^{1}$H NMR (300 MHz, $CDCl_3$) δ 8.57 (s, 1H), 8.13 (d, $J$ = 2.1 Hz, 1H), 7.89 (d, $J$ = 10.4 Hz, 1H), 7.62 (s, 2H), 7.07 (d, $J$ = 10.4 Hz, 1H). $^{13}$C NMR (75 MHz, $CDCl_3$) δ 178.60, 137.93, 135.67, 134.50, 133.42, 131.95, 128.36, 128.23, 125.77.

#### (+)-6-Chloro-4*H*-thiochromen-4-one 1-oxide (7f)

Yield 75%. $[\alpha]_D^{25} = +65.9^{\circ}$ (c = 20 mg/mL in chloroform). $^{1}$H NMR (300 MHz, $CDCl_3$) δ 8.58 (s, 1H), 7.89 (d, $J$ = 10.5 Hz, 1H), 7.63 (s, 2H), 7.08 (d, $J$ = 10.5 Hz, 1H).

#### (−)-6-Chloro-4*H*-thiochromen-4-one 1-oxide (7g)

Yield 75%. $[\alpha]_D^{25} = -35.1^{\circ}$ (c = 20 mg/mL in chloroform). $^{1}$H NMR (300.

### 2.14. General procedure VI

#### 2-Methylthiochroman-4-one (9a)

Thiophenol **1a** (100 mg, 0.907 mmol) and crotonic acid (93.0 mg, 1.08 mmol) were dissolved in dry ACN (5 mL). A catalytic amount of TBAF was added and the solution was heated at 100 °C overnight. The reaction mixture was quenched with brine (25 mL) and extracted with ethyl acetate (3 × 25 mL), and the organic layer was concentrated under reduced pressure, resulting in the formation of a yellowish oil (151.306 mg, 0.771 mmol), which was cooled to 0 °C in an ice bath. Concentrated sulfuric acid (5 mL) was then added and the reaction mixture was stirred for 10 min at 0 °C, warmed to RT, and stirred for another 24 h. The reaction mixture was quenched with ice and extracted with DCM (3 × 25 mL). The combined organic layers were washed with water (25 mL) and

saturated $NaHCO_3$ solution (25 mL). The combined organic layers were dried over $Na_2SO_4$ and concentrated under reduced pressure. The residue was purified via silica gel column chromatography using hexane:EtOAc (4:1) as an eluent to produce the pure compound **9a** (110 mg, 0.617 mmol) as a yellowish oil with a yield of 80%.

$^1$H NMR (300 MHz, $CDCl_3$) δ 8.12 (dd, $J$ = 1.2, 7.9 Hz, 1H), 7.39 (d, $J$ = 1.5 Hz, 1H), 7.30 (d, $J$ = 0.6 Hz, 1H), 7.25 (d, $J$ = 14.7 Hz, 1H), 3.08 (dd, $J$ = 3.1 Hz, 2H), 2.82 (dd, $J$ = 3.1 Hz, 2H), 1.47 (d, $J$ = 6.8 Hz, 3H). $^{13}$C NMR (75 MHz, $CDCl_3$) δ 194.73, 141.84, 133.52, 132.89, 130.36, 128.99, 127.51, 124.95, 77.54, 77.12, 76.70, 47.84, 36.45, 20.49. HRMS–ESI *m/z* for $C_{11}H_9O_3S$ $[M+H]^+$, calculated: 291.0149 and observed: 291.0144.

This procedure was used to synthesize compounds **9a–c**.

Compounds **11a–c** were synthesized from **10a–c** according to general procedure III.

**2-Methyl-4*H*-thiochromen-4-one 1,1 dioxide (11a)**

Yield 65%. $^1$H NMR (300 MHz, $CDCl_3$) δ 8.24 (d, $J$ = 7.8 Hz, 1H), 8.12 (d, $J$ = 7.8 Hz, 1H), 7.86 (m, $J$ = 9.5 Hz, 1H), 7.31 (s, 1H), 6.60 (d, $J$ = 1.6 Hz, 1H), 2.50 (d, $J$ = 1.7 Hz, 3H). $^{13}$C NMR (75 MHz, $CDCl_3$) δ 177.72, 152.38, 140.96, 134.62, 133.01, 129.84, 128.68, 128.31, 123.63, 14.12. HRMS–ESI *m/z* for $C_{10}H_8O_3SNa$ $[M+Na]^+$, calculated: 231.0091 and observed: 231.0086.

**2-Hepthylthiochromen-4-one 1,1 dioxide (11b)**

Yield 68%. $^1$H NMR (300 MHz, $CDCl_3$) δ 8.23 (dd, $J$ = 1.0, 7.8 Hz, 1H), 8.11 (t, $J$ = 4.0 Hz, 1H), 7.85 (m, $J$ = 4.5 Hz, 1H), 7.31 (s, 1H), 6.59 (t, $J$ = 1.5 Hz, 1H), 2.67 (s, 1H), 2.22 (s, 1H), 1.68 (s, 1H), 1.32 (s, 1H), 0.93 (t, $J$ = 6.6 Hz, 1H). $^{13}$C NMR (75 MHz, CDCl3) δ 177.95, 156.46, 141.21, 134.61, 128.62, 128.60, 123.55, 31.65, 28.97, 28.88, 27.21, 27.19, 22.61, 14.10. HRMS–ESI *m/z* for $C_{16}H_{20}O_3SNa$ $[M+Na]^+$, calculated: 315.1030 and observed: 315.1029.

**2-Nonethylthiochromen-4-one 1,1 dioxide (11c)**

Yield 65%. $^1$H NMR (300 MHz, $CDCl_3$) δ 8.21 (d, $J$ = 7.9 Hz, 1H), 8.09 (d, $J$ = 7.9 Hz, 1H), 7.83 (m, $J$ = 4.9 Hz, 1H), 6.58 (s, 1H), 2.81 (q, $J$ = 5.2 Hz, 1H), 1.80 (m, $J$ = 7.5 Hz, 1H), 1.46 (d, $J$ = 20.6 Hz, 1H), 0.92 (t, $J$ = 6.2 Hz, 1H). $^{13}$C NMR (75 MHz, $CDCl_3$) δ 177.97, 156.50, 141.213, 134.61, 132.93, 128.65, 128.60, 128.23, 123.57, 31.86, 29.42, 29.61, 29.22, 29.02, 27.16, 22.69, 14.15. HRMS–ESI *m/z* for $C_{18}H_{25}O_3SNa$ $[M+Na]^+$, calculated: 343.1343 and observed: 343.1336.

*2.15. General procedure VII*

**3-(2-Chlorobenzyl)-4*H*-thiochromen-4-one (13a)**

Solutions of thiochroman-4-one **3a** (200 mg, 1.22 mmol), 4-chlorobenzaldehyde (205 mg, 1.46 mmol), and piperidine (200 μL, 1.46 mmol) in EtOH (5 mL) were treated with a catalytic amount of LiBr (5.0 mg, 0.06 mmol). The tubes were sealed and heated under microwave irradiation at 100 °C for 1 h under argon atmosphere. The reaction progression was monitored by TLC. The reaction mixture was quenched with brine (25 mL) and extracted with ethyl acetate (4 × 20 mL). The combined organic layers were dried over anhydrous $Na_2SO_4$. The solvent was removed under vacuum, and the residue was washed with cold EtOH:water (1:1, 25 mL). Vacuum filtration resulted in the formation of the compound **13a** (301 mg, 1.159 mmol) as a white solid with a yield of 95%.

$^1$H NMR (300 MHz, $CDCl_3$) δ 8.65 (d, $J$ = 7.5 Hz, 1H), 7.61 (m, 2H), 7.59 (m, $J$ = 7.9 Hz, 1H), 7.43 (q, $J$ = 5.8 Hz, 3H), 7.27 (m, $J$ = 6.0 Hz, 2H), 4.17 (s, 2H). $^{13}$C NMR (75 MHz, $CDCl_3$) δ 179.01, 137.27, 136.42, 134.67, 134.60, 134.20, 131.99, 131.58, 131.10, 129.78, 129.08, 128.27, 127.56, 127.14, 126.50, 35.47.

Compounds **14a–d** were synthesized from **13a–d** according to general procedure II.

**3-(2-Chlorobenzyl)-4*H*-thiochromen-4-one 1,1-dioxide (14a)**

Yield 60%. $^1$H NMR (300 MHz, $CDCl_3$) δ 8.31 (dd, $J$ = 1.1, 7.9 Hz, 1H), 8.07 (dd, $J$ = 3.9, 3.9 Hz, 1H), 7.90 (dt, $J$ = 1.3, 7.6 Hz, 1H), 7.81 (dt, $J$ = 1.3, 7.7 Hz, 1H), 7.52–7.46 (m,1H), 7.38–7.34 (m, 3H), 6.76 (t, $J$ = 1.7 Hz, 1H), 4.08 (d, $J$ = 1.7 Hz, 2H). $^{13}$C NMR (75 MHz, $CDCl_3$) δ 178.35, 143.05, 140.96, 136.74, 134.81, 134.68, 133.15, 133.05, 132.03, 130.26, 129.41, 128.97, 128.41, 127.60, 123.35, 34.24. HRMS–ESI *m/z* for $C_{16}H_{12}O_3SCl$ $[M+H]^+$, calculated: 319.0195 and observed: 319.0190.

**3-(4-Chlorobenzyl)-4*H*-thiochromen-4-one 1,1-dioxide (14b)**

Yield 84%. $^1$H NMR (300 MHz, acetone) δ 8.22 (d, $J$ = 8.2 Hz, 1H), 7.97 (m, $J$ = 5.1 Hz, 3H), 7.41 (s, 4H), 3.98 (d, $J$ = 1.5 Hz, 3H), 2.06 (m, $J$ = 2.2 Hz, 1H). $^{13}$C NMR (75 MHz, acetone) δ 178.26, 144.10, 141.36, 137.35, 135.67,133.26, 132.40, 131.17, 128.77, 128.49, 128.36, 123.05, 35.43. HRMS–ESI *m/z* for $C_{16}H_{12}O_3SCl$ $[M+H]^+$, calculated: 319.0195 and observed: 319.0190.

**3-(4-Chlorobenzyl)-4*H*-thiochromen-4-one 1,1-dioxide (14c)**

Yield 90%. $^1$H NMR (300 MHz, $CDCl_3$) δ 8.25 (d, $J$ = 7.8 Hz, 1H), 7.88 (m, $J$ = 9.5 Hz, 9H), 7.42 (d, $J$ = 8.2 Hz, 2H), 7.00 (s, 1H),

3.99 (s, 2H). $^{13}$C NMR (75 MHz, $CDCl_3$) δ 178.08, 143.24, 140.95, 140.85, 137.49, 135.05, 133.29, 132.85, 130.33, 129.02, 128.11, 123.41, 118.50, 111.61, 36.86. HRMS–ESI *m/z* for $C_{17}H_{12}NO_3S$ $[M+H]^+$, calculated: 310.0537 and observed: 310.0531.

**3-(4-Trifluorobenzyl)-4*H*-thiochromen-4-one 1,1-dioxide (14d)**

Yield 88%. $^1$H NMR (300 MHz, $CDCl_3$) δ 8.27 (d, $J = 7.8$ Hz, 2H), 8.06 (d, $J = 7.6$ Hz, 2H), 7.91 (t, $J = 7.7$ Hz, 2H), 7.81 (t, $J = 7.7$ Hz, 2H), 7.68 (d, $J = 8.0$ Hz, 4H), 7.59 (d, $J = 8.5$ Hz, 1H), 7.49 (d, $J = 8.5$ Hz, 1H), 7.42 (d, $J = 8.8$ Hz, 4H), 6.93 (s, 2H), 4.00 (s, 3H). $^{13}$C NMR (75 MHz, $CDCl_3$) δ 178.22, 143.90, 140.91, 139.33, 137.25, 134.94, 133.23, 129.97, 129.25, 129.01, 128.24, 126.21, 126.16, 126.11, 126.06, 123.38, 36.50. HRMS–ESI *m/z* for $C_{17}H_{12}F_3O_3S$ $[M+H]^+$, calculated: 353.0459 and observed: 353.0450.

Compounds **17a–b** were synthesized from **16a–b** according to general procedure II.

**3-(Furan-2-yl-methyl)-4*H*-thiochromen-4-one 1,1-dioxide (17a)**

Yield 67%. $^1$H NMR (300 MHz, $CDCl_3$) δ 8.29 (dd, $J = 0.9$, 7.9 Hz, 1H), 8.07 (d, $J = 7.8$ Hz, 1H), 7.91 (m, $J = 3.3$ Hz, 1H), 7.81 (m, $J = 3.3$ Hz, 1H), 7.46 (d, $J = 1.1$ Hz, 1H), 7.02 (t, $J = 1.6$ Hz, 1H), 6.43 (dd, $J = 1.9$, 3.1 Hz, 1H), 6.31 (d, $J = 3.1$ Hz, 1H), 4.00 (s, 2H). $^{13}$C NMR (75 MHz, $CDCl_3$) δ 178.18, 148.40, 142.97, 142.00, 141.03, 137.03, 134.84, 133.14, 128.92, 123.37, 110.87, 109.34, 29.01. HRMS–ESI *m/z* for $C_{14}H_{11}O_4S$ $[M+H]^+$, calculated: 275.0378 and observed: 275.0376.

**3-(Thiophen-2-yl-methyl)-4*H*-thiochromen-4-one 1,1-dioxide (17b)**

Yield 65%. $^1$H NMR (300 MHz, $CDCl_3$) δ 8.29 (q, $J = 3.0$ Hz, 1H), 8.06 (q, $J = 2.9$ Hz, 1H), 7.91 (m, $J = 3.3$ Hz, 1H), 7.80 (m, $J = 3.3$ Hz, 1H), 7.63 (m, $J = 2.3$ Hz, 1H), 7.32 (t, $J = 2.6$ Hz, 1H), 7.31 (s, 1H), 7.03 (m, $J = 3.0$ Hz, 1H), 4.15 (d, $J = 0.9$ Hz, 2H). $^{13}$C NMR (75 MHz, $CDCl_3$) δ 178.78, 144.16, 141.00, 136.96, 136.22, 134.47, 133.15, 128.93, 128.36, 127.94, 127.64, 125.88, 123.36, 30.45. HRMS–ESI *m/z* for $C_{14}H_{11}O_3S_2$ $[M+H]^+$, calculated: 291.0149 and observed: 291.0144.

*2.16. General procedure VIII*

**6-(3,5-Bis(trifluoromethyl)phenyl)thiochroman-4-one (19a)**

The solutions of 7-bromothiochroman-4-one **3d** (50.0 mg, 0.205 mmol) and $Et_3N$ (90 μL, 0.647× mmol) in water:DME (2:1 v/v%, degassed) were added into an oven-dried Schlenk flask filled with argon. Following the addition of **18a** (65.0 mg, 0.252 mmol) and Pd(dppf)$Cl_2$ (9.0 mg, 0.011 mmol, 5 mol%), the mixture was heated at 50 °C for 10 min. A catalytic amount of the ligand (L1: 2-amino-pyrimidine-4,6-diol) (0.0025 M solution in water, 1.0 mL; 0.317 mg, 0.0025 mmol). After 48 h at 80 °C, the coupling reaction was completed, as verified using TLC. The reaction mixture was quenched with 1 N HCl (5 mL) and extracted with ethyl acetate (4 × 20 mL). The combined organic phases were washed with brine (3 × 25 mL), dried over $MgSO_4$, filtered, and evaporated. Flash chromatography on silica gel (pentane:ethyl acetate, 6:1) produced the cross-coupling compound **19a** as a white solid (43.3 mg, 0.115 mmol) with a yield of 56%.

$^1$H NMR (500 MHz, $CDCl_3$) δ 8.18 (d, $J = 8.3$ Hz, 1H), 7.60 (t, $J = 4.7$ Hz, 2H), 7.50 (s, 1H), 7.46 (t, $J = 7.5$ Hz, 2H), 7.41 (m, $J = 4.5$ Hz, 2H), 3.28 (t, $J = 6.4$ Hz, 2H), 3.01 (t, $J = 6.4$ Hz, 2H). $^{13}$C NMR (125 MHz, $CDCl_3$) δ 26.71, 39.47, 121.00, 122.09, 124.08, 124.26, 126.22, 127.36, 130.52, 130.78, 132.70, 141.48, 142.72, 143.47, 193.45. IR $\nu$ ($cm^{-1}$) 3067, 1667, 1377, 1275, 705, 681. HRMS–ESI *m/z* for $C_{17}H_{10}OF_6S$ $[M+H]^+$, calculated: 377.04293 and observed: 377.04322.

This methodology was used to synthesize compounds **19a–e.**

Compounds **20a–e** were synthesized from **19a–e** according to general procedure II.

Compounds **21a–e** were synthesized from **20a–e** according to general procedure III.

**6-(3,5-Bis(trifluoromethyl)phenyl) 4 *H*-thiochromen-4-one 1,1-dioxide (21a)**

Yield 90%. $^1$H NMR (300 MHz, $CDCl_3$) δ 8.47 (d, $J = 1.7$ Hz, 1H), 8.25 (d, $J = 8.1$ Hz, 1H), 8.18 (dd, $J = 1.9$, 8.3 Hz, 1H), 8.13 (s, 2H), 8.03 (s, 1H), 7.51–7.46 (m, 1H), 6.91–6.86 (m, 1H). $^{13}$C NMR (75 MHz, $CDCl_3$) δ 177.53, 143.06, 140.85, 140.15, 133.41, 133.16, 132.71, 132.35, 128.88, 127.54, 127.13, 124.90, 124.82, 122.94, 121.20. HRMS–ESI *m/z* for $C_{17}H_9O_3F_6S$ $[M+H]^+$, calculated: 407.0176 and observed: 407.0165.

**7-(3,5-Bis(trifluoromethyl)phenyl)-4*H*-thiochromen-4-one 1,1-dioxide (21b)**

Yield 96%. $^1$H NMR (300 MHz, $CDCl_3$) δ 8.39 (d, $J = 8.3$ Hz, 1H), 8.31 (d, $J = 1.7$ Hz, 1H), 8.15 (s, 1H), 8.05 (dd, $J = 1.8$, 8.2 Hz, 1H), 7.49 (d, $J = 12.1$ Hz, 1H), 7.31 (s, 1H), 6.87 (d, $J = 11.6$ Hz, 1H). $^{13}$C NMR (75 MHz, $CDCl_3$) δ 177.29, 144.80, 142.03, 139.87, 139.87, 13321, 132.77, 132.53, 131.60, 129.79, 127.81, 127.59, 122.24, 121.17.

**8-(3,5-Bis(trifluoromethyl)phenyl)-4*H*-thiochromen-4-one 1,1-dioxide (21c)**

Yield 95%. $^1$H NMR (300 MHz, $CDCl_3$) δ 8.40 (dd, $J = 1.3$, 8.0 Hz, 1H), 8.03 (s, 1H), 7.88 (t, $J = 7.8$ Hz, 1H), 7.72 (dd, $J = 1.3$, 7.6

Hz, 1H), 7.31 (s, 1H), 6.80 (d, $J = 11.4$ Hz, 1H). $^{13}$C NMR (75 MHz, $CDCl_3$) δ 177.84, 141.55, 138.30, 137.75, 137.69, 132.62, 131.48, 131.01, 130.59, 129.36, 128.92, 124.94, 122.83, 121.32. HRMS–ESI *m/z* for $C_{17}H_8O_3F_6SNa$ $[M+Na]^+$, calculated: 428.9996 and observed: 428.9985.

**6-Phenyl-4*H*-thiochromen-4-one 1,1-dioxide (21d)**

Yield 85%. $^1$H NMR (300 MHz, $CDCl_3$) δ 8.30 (q, $J = 3.9$ Hz, 1H), 8.01 (q, $J = 3.4$ Hz, 1H), 7.58 (m, $J = 7.1$ Hz, 1H), 7.31 (s, 1H), 6.83 (d, $J = 11.6$ Hz, 1H). $^{13}$C NMR (75 MHz, $CDCl_3$) δ 177.67, 148.19, 141.47, 140.42, 137.65, 132.62, 131.35, 129.71, 129.43, 129.33, 127.40, 121.82. HRMS–ESI *m/z* for $C_{17}H_{10}OF_6S$ $[M+H]^+$, calculated: 271.0428 and observed: 271.0422.

**6-Phenyl-4*H*-thiochromen-4-one 1,1-dioxide (21e)**

Yield 95%. $^1$H NMR (300 MHz, $CDCl_3$) δ 8.31 (q, $J = 3.1$ Hz, 1H), 7.80 (t, $J = 7.7$ Hz, 1H), 7.71 (q, $J = 3.0$ Hz, 1H), 7.53 (m, $J = 2.4$ Hz, 1H), 7.25 (d, $J = 11.3$ Hz, 1H), 6.76 (d, $J = 11.3$ Hz, 1H). $^{13}$C NMR (75 MHz, $CDCl_3$) δ 175.56, 142.15, 141.43, 138.56, 138.29, 136.56, 132.13, 128.79, 130.68, 130.08, 128.81, 128.24, 127.85. HRMS–ESI *m/z* for $C_{17}H_{10}OF_6S$ $[M+H]^+$, calculated: 271.0428 and observed: 271.0419.

## 3. Results and discussion

The compounds synthetized by Vargas. E et al. [9], resulted in increased *in vitro* activity against intracellular amastigotes of *L. panamensis* (LC = 3.24 μM, selectivity index = 173.24). These compounds carry a sulfone group that reacts electronically with a carbonyl group via a double bond and two substituted aromatic rings comprising electron-withdrawing groups such as fluor and trifluoromethyl. This compound, presented as **R1** in Fig. 1, is an isostere of the naphthoquinones. The present study provides evidence that the action mode of **R1** involves the parasite redox pathway.

The possible role of TR, a reductase, as an electron sink that enables interaction between TR and compounds **R1–4** was examined. For this purpose, a short electrochemical experiment was designed to test the ability of the molecules to donate or receive electrons. Considering the fact that quinone redox behavior is generally examined using CV under a broad set of conditions, we tested the hypothesis that the 4H-thiochromen-4-one 1,1-dioxide core is electrochemically unactive and has a voltammogram different to that of a quinone. A simple system consisting of ACN as the solvent and a TBAB-like support electrolyte at a concentration of 0.1 M was used. Further, a scan was performed with a large potential window ranging from −1.5 to 2.5 V at a rate of 150 mV/s(Fig. 2). Similarly, another study focused on the potential biological plot between 0.1 and 1 V, Finally, as an experimental control, the redox behavior of p-quinone was determined under the abovementioned conditions; the results are presented in Fig. 2. Where two peaks can be observed due to anodic (oxidation) and cathodic currents (reduction). The electrochemical events produced at low potential ranges play a critical role as they are involved in some relevant biochemical processes such as the redox reaction of NADH and FADH associated with the catalytic action of TR. After determining the optimal conditions for the electrochemical assessment, target compounds **6a** and **R2** were exposed to cyclical cathodic and anodic currents in the low potential range. These result, which revealed the unexpected capacitive behavior of the compounds. In other words, the molecules accumulated charge, and an electron transfer with low potential was detected in the experiment, indicating their biological effect. These results suggest that the use of thiochromen-4-one-1,1-dioxide as an isostere of quinone presents an entirely different electric behavior with inconsistencies in redox characteristics. For this reason, the biochemical mechanism of action involving electron chain disruption in TR between the electron source NADH and catalytic center induced by the **R1** core (and similar compounds) could not be successful. In other words, the mechanism of action involves another type of interaction as these cores are electrochemically inactive.

Once it was established that the core does not present any redox potential, a relatively indirect test was performed in the redox Leishmania pathway.

The results presented in Fig. 3 indicate a strong oxidative burst after 1 h, which is similar to that observed in rotenone (**ROT**) control, a mitochondrial respiratory chain disruptor [21]. Unexpectedly, the tested compounds produced higher ROS levels than glucantime, meglumine antimoniate, or antimony trivalent (**Sb III**). Although there are several treatments that induce the production of ROS, the extent of disturbance to the system that controls ROS remains unknown. To this end, a parametrization was performed and the results were plotted in Fig. 4, which clearly indicates that **ROT** plays an irrelevant role in thiochromen-4-one compounds, suggesting that parasites exposed to these compounds cannot balance the ROS levels produced. This results in a disruption of the homeostasis equilibrium, leading to the parasite death (see Fig. 5).

Another complementary study on ROS effect reported the measurement of mitochondrial function. Tetramethylrhodamine

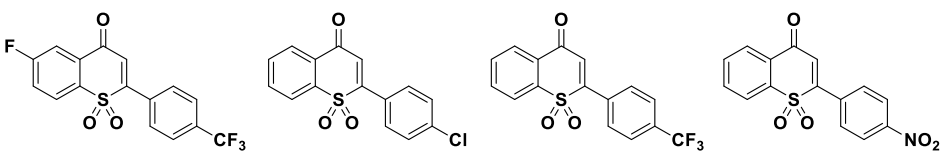


**Fig. 1.** Reference compounds used like positive control (from left to right): R1, R2, R3, R4, respectively.

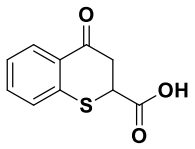


**Fig. 2.** Reference compound used like negative control.

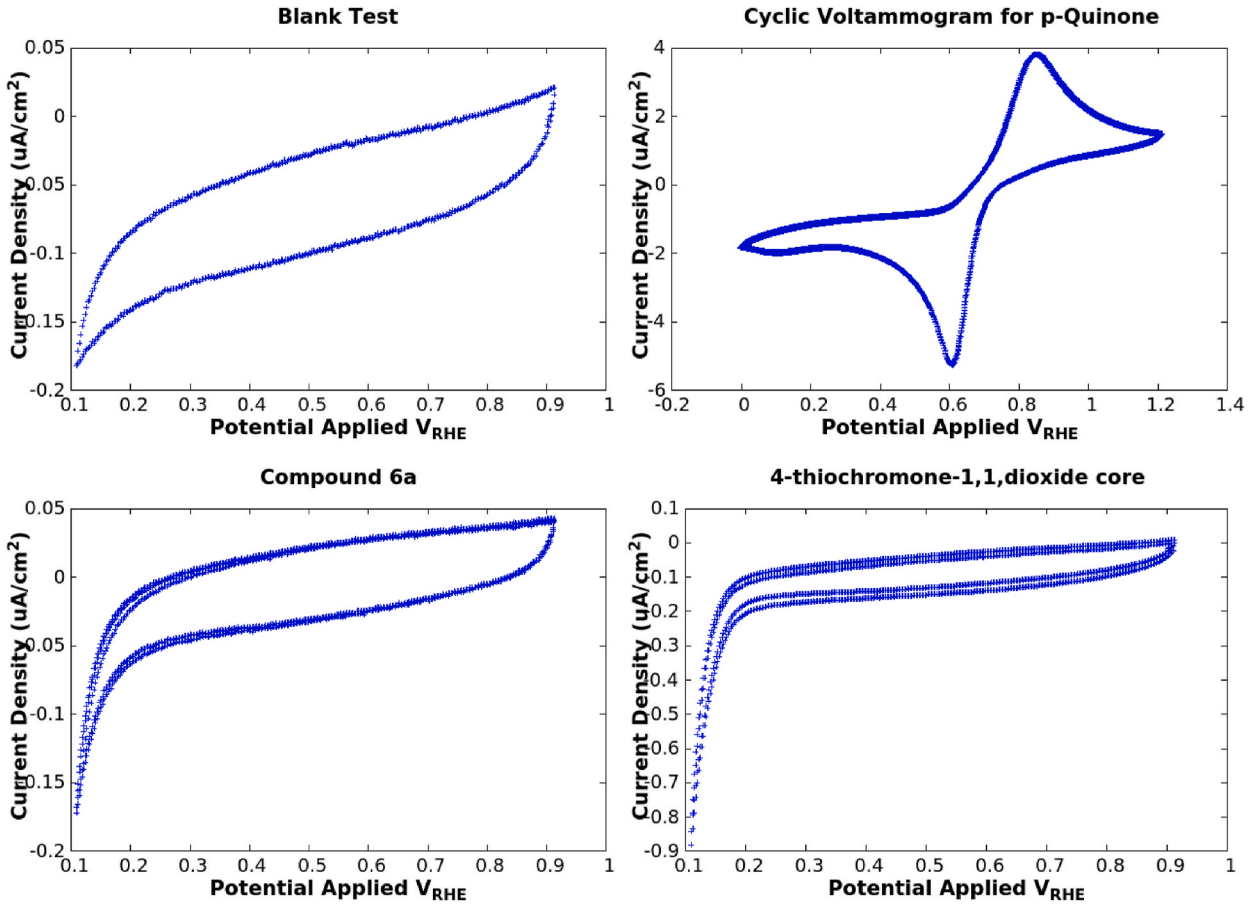


**Fig. 3.** Electrochemical measures over scaffold core and R2.

(TMRM) was used to determine the mitochondrial index function as it accumulates in functional mitochondrial cells and develops a color when there is any disturbance in the mitochondrial membrane potential. This staining was performed on amastigotes released from *L. braziliensis* WT 1 h after treatment to determine the $EC_{90}$ for each treatment. Residual TMRM was then quantified using a flow cytometer.

This graph (Fig. 4) presents a similar effect to that observed with sodium cyanide, a common reversible inhibitor of the mitochondrial cytochrome oxidase that blocks electron transport, resulting in decreased oxidative metabolism and oxygen utilization. Further, NaCN is a reducing agent that can react with the thiol groups of a protein [22] demonstrating its efficacy at the mitochondrial level; this may be due to redox pathway inhibition, leading to the assumption that ROS accumulation results from its metabolic production.

### *3.1. Biological activity*

After it was revealed that the nucleus of thiochromone 1,1 dioxide affects the cell viability of parasites via the accumulation of ROS, a series of compounds derived from the base nucleus were synthesized, conserving the elements of the pharmacophore to establish a structure–activity relationship.

Furthermore, considering the fact that *Trypanosoma* and *Leishmania* belong to the same taxonomic family and share the same

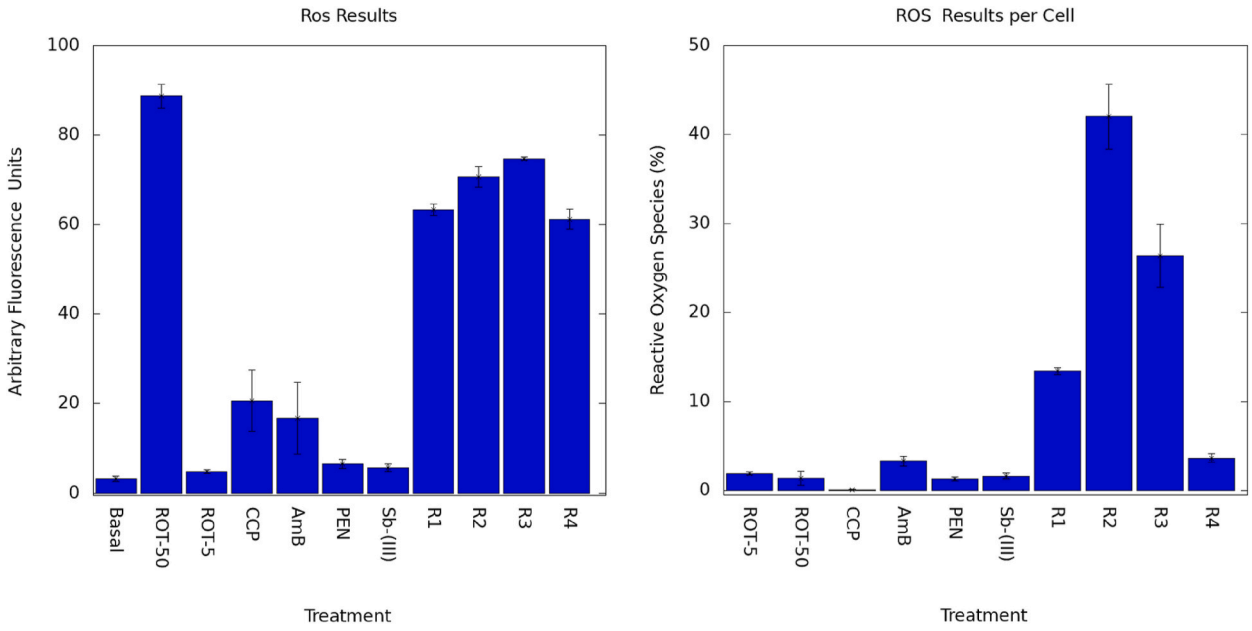


**Fig. 4.** Indirect biological effects of reference compounds on the trypanothione system.

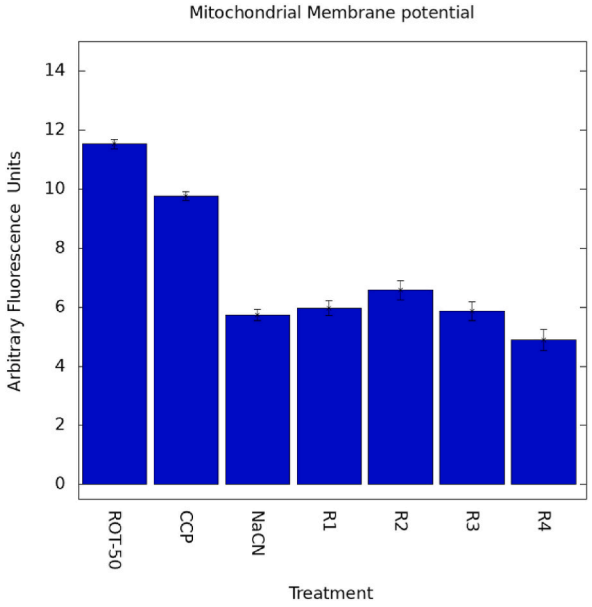


**Fig. 5.** Biological effect on parasite mitochondrial membrane potential.

metabolic pathway of TR as well as orthology of glutathione reductase, which is a host enzyme that is shared with *Plasmodium*, a series of compounds were assessed on these parasites to determine the effect of these class of compounds on redox mechanisms.

The experiments that evaluated the antileishmanial activity of compounds showed that compounds **11a**, **11b**, **14c**, and **21c** exhibit the highest activities, allowing the establishment of the following relationships.

Series **6** compounds consist of simple variations of the base nucleus (**6a**), involving modifications of hydrogen atoms by halogens F (**6b**), Cl (**6b**), and Br (**6d**). These modifications did not cause a significant impact when the type of substituent was altered in the biological models assessed. However, alteration in position of the bromine atom (**6d–f**) led to an activity cliff in the trypanosome model, suggesting that the positions closest to the sulfur atom are particularly sensitive. Moreover, the presence of electron-attracting substituents, without an increase in the polar area, does not affect the increased activity.

Series **7** compounds, including the racemic (**7a, 7d,** and **7e**) and chiral (**7b, 7c, 7f,** and **7g**) sulfoxides, did not show any significant

biological difference; therefore, the structural derivatives can be proposed without considering the asymmetric center. Another fact is the differences between sulfoxides and sulfones (**6a** and **7a, 6b** and **7d, 6c** and **7e**). Based on these results, it is clear that the trypanosome biological model is sensitive to these modifications, thus sulfoxides are more active in this biological model than in other models, which remain unaffected.

Series **11** compounds, which are synthesized after substituting position 1 of the ring to obtain a linear chain, exhibit increased activity; however, this activity decreases as the chain elongates. Short and extremely long chains lost their activity, indicating that an increased area is a structural requirement of these compounds. However, compound **11b** unexpectedly resulted in increased biological activity against all three biological models.

Another important structural relationship is observed in the compounds of series 14 and 21, which exhibit a significant loss of activity when the aromatic groups deactivated by the trifluoromethyl substituent it moves away from the atom sulfur atom **(21d and 21e)**. This effect is weaker in the other biological models. But in contrast, the biological activity on the Plasmodium model is highest when the strong electron-attracting groups are removed from the sulfur center **(21a)**. This experimental finding is significant as it demonstrates the structural differences in the enzyme, allowing the systematic control of selectivity.

Overall, it is possible to confirm that substituents with strong electron-attracting character, which is associated with an increase in polar area and close proximity to the heterocycle and sulfone group, is the most effective combination in the three biological models evaluated (**14d** and **21c**).

On the other hand, the results obtained when evaluating the cytotoxicity of the compounds synthesized on human cell lines U-937 show that, although in most cases the same order of magnitude is obtained as the bioactivity, the selectivity varies or increases depending on the pathogen evaluated. Additionally, it is observed that the selectivity increases with the change of the type of substituent, **(14b-14c)** or, with the change of position **(21c-21D).** Additionally, considering the reported cytotoxicity of the compounds illustrated in Fig. 1, which have been used as positive controls, allows us to infer that although the interaction with other systems such as glutathione reductase cannot be ruled out, it can be modulated with small structural changes, which allows us to maintain the hypothesis of allosteric modulation of TR (see Fig. 6).

### *3.2. In silico analysis*

To hypothesize over possible action mechanism (MOA) of this class compounds and postulated new set of chemical modification, a docking molecular experiment was performed limited to rectangular grid box shown in Fig. 7, with the center of the box indicated along with the catalytic center of the enzyme (see Table 1).

The results of affinity energy bonding in all compounds are summarized in Fig. 8, providing essential information about trends of interaction Ligand-TR; the green and violet boxes represent the scores of algorithms (Swiss dock and Autodock, respectively such as the reference (**R1–4**) compounds, were considered as candidates for significant antileishmanial activity, previously reported [9], and **R5** is the negative control due to low bioactivity [23]. This graph shows that series **6a–f** presents a similar performance to that of **R5**; however, series **14a–d**, **17a–b**, and **21a–d** present a similar or better affinity compared with the reference series (**R1–4**). This result demonstrates a good correlation between the experimental and theoretical results, thus providing important information regarding the most important amino acids involved in the inhibitory activity, such as Ser-14, Leu-17, Trp-21, Ser-109, Tyr-110, and Met-113. The correlated between key amino acids, interaction and distance with bioactivity is summarized in Table 2.

These residues are affected by the distance as well as type of interaction, degrees of freedom, and polar area. In case of **R4**, it is clear that its acidic property leads to strong polarizability as well as van der Waals interactions, which is disadvantage concerning to the apolar character of the most relevant residues into the allosteric receptor Therefore, the affinity between ligand **R4** and the receptor is relatively weak to produce an inhibitory effect.

As presented in Fig. 8, the hydrogen bond between Ser-109 and side ring in the compounds (**14d** and **21c**) is essential for their affinity energy bonding (Fig. 7) and biological effects; Thus the interaction within an allosteric receptor formed by helix residues 14–21 interspersed with another helix of domain (I), formed by residues 106–113, and the helix contributed by domain (III) could disrupt the normal allosteric receptor conformation and configuration, resulting in higher interhelical forces that dislodge the catalytic center formed by Cys52 and Cys57 (Fig. 10) For these reasons thiochromen-4-one 1,1-dioxide and its derivatives are allosteric inhibitors of TR (see Fig. 9). In consequence, the biological target important features are hydrophobicity, high electron density and high conservation of amino acid sequence, are essential to design compounds can be considered as promising therapeutics alternatives.

## 4. Conclusions

This proposed chemical modifications of the **R1** core that led to the discovery of a lead compound with a suitable bioactive profile against leishmaniasis, trypanosomiasis, and malaria.

So far, an allosteric receptor and its general features, such as electronic density and conservation and polarity of amino acid sequences, have been described as critical parameters for designing novel compounds. This strategy was in accordance with the fact that substituents that were incorporated in the thiochromane core and their derivatives, with electron-withdrawing groups and low polarizability, showed the most effective biological effects. Moreover, complementary biological studies were conducted to elucidate the potential mode of action. Indirect measurements of the tryparedoxin system revealed a significant increase in the ROS levels and robust mitochondrion perturbation of the dead parasites. Thus, the principal hypothesis was confirmed; 4H-thiochromen-4-one 1,1-dioxide can disrupt important metabolic pathways that are essential for ROS control. However, following a completely different procedure in the voltametric analyses than that followed for their isosteric analogous compounds revealed that the thiochromone core

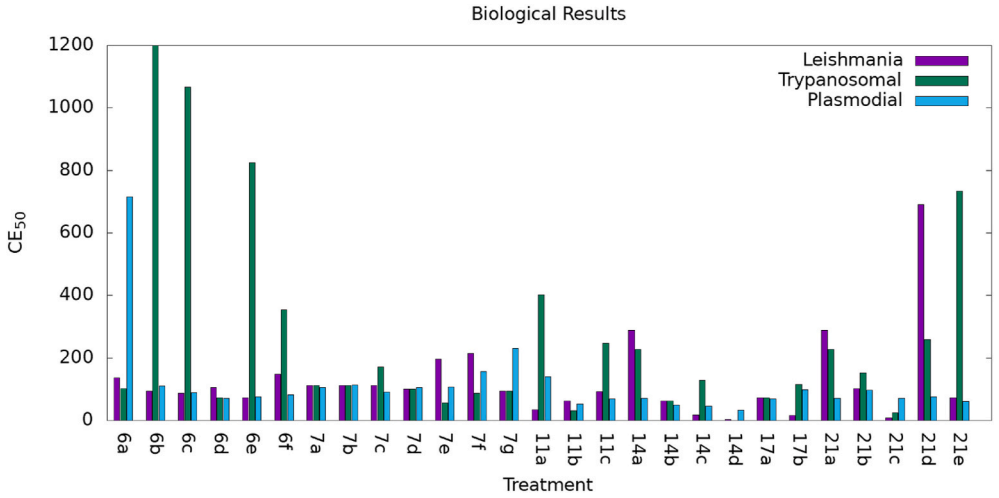


**Fig. 6.** Biological effect of the derivatives compounds on three biological models.

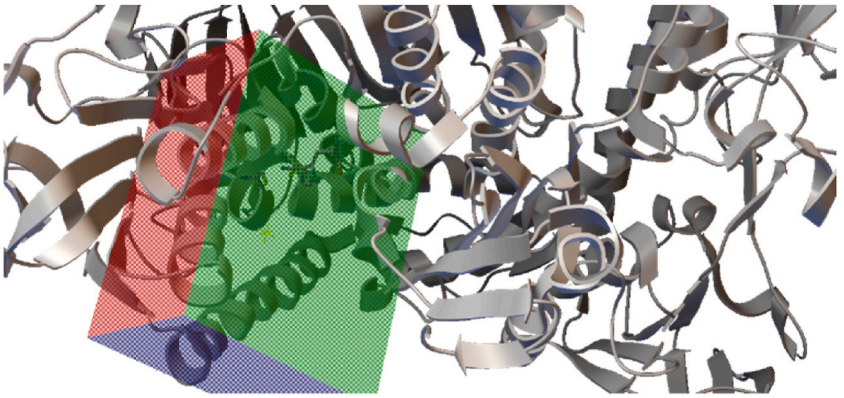

**Fig. 7.** Delimited zone to molecular docking simulation.

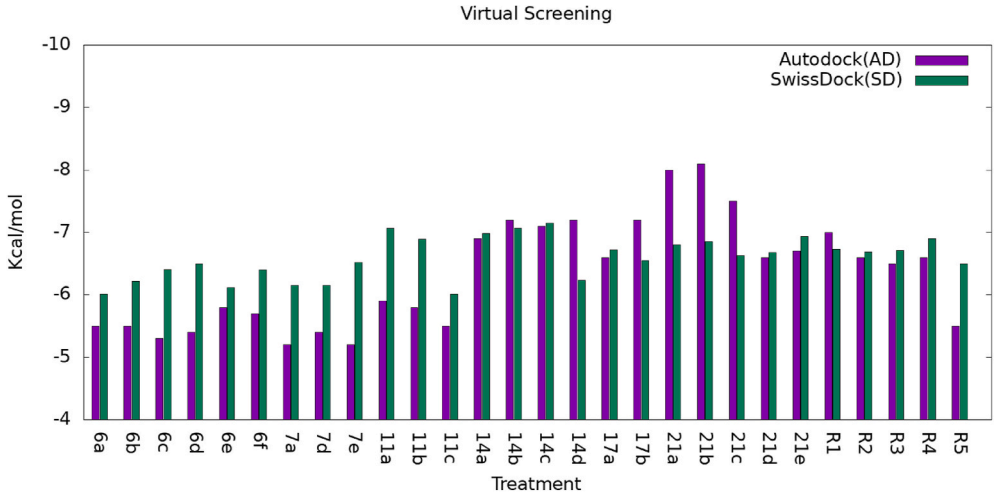


**Fig. 8.** Determination of affinity between ligand and enzyme via molecular docking.

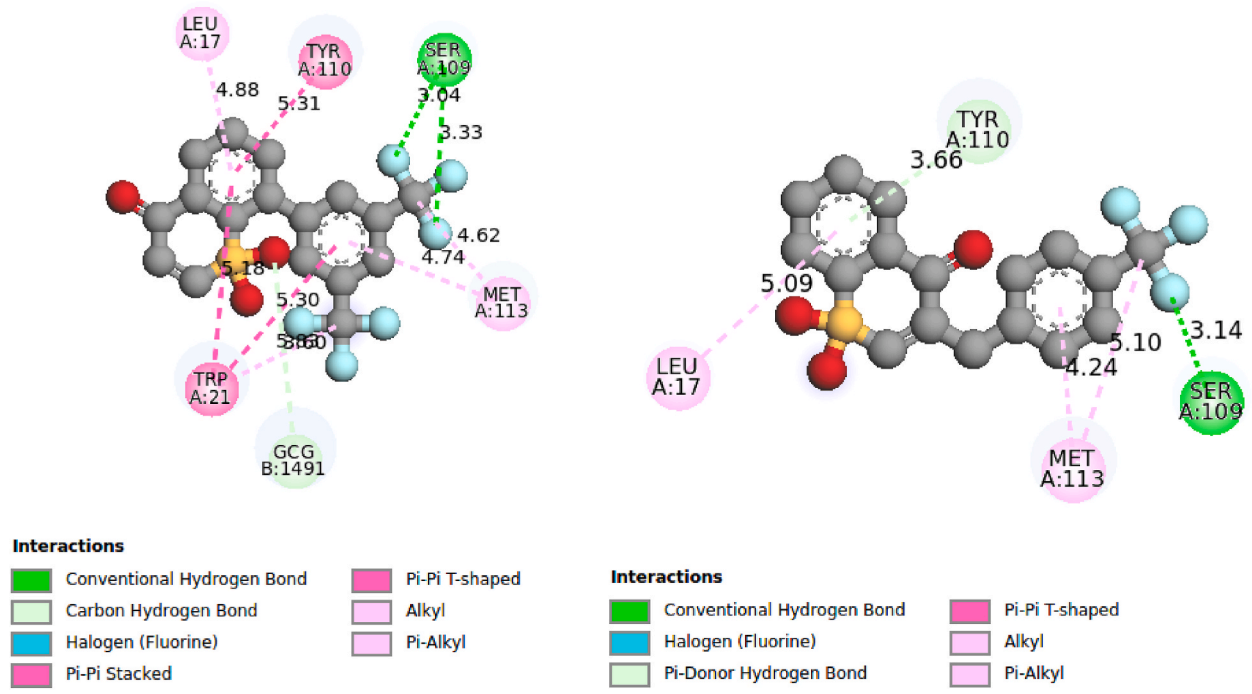


**Fig. 9.** Best fit and enzyme interaction in compounds **21c** and **14d**.

**Table 1**
Biological results of the derivatives compounds.

| Compound | Cytotoxicity | | Leishmanial | | IS | Trypanosomal | | IS | Plasmodial | | IS |
|---|---|---|---|---|---|---|---|---|---|---|---|
| | $CL_{50}$ (μM) | SD | $CE_{50}$ (μM) | SD | | $CE_{50}$ (μM) | SD | | $CE_{50}$ (μM) | SD | |
| **6a** | 1029.8 | 0 | 137.26 | 2.44 | 7.50 | 102.9 | <10 | 10 | 716.98 | 84.92 | 1.44 |
| **6b** | 274.83 | 10.05 | 94,26 | <2.9 | 2.92 | 1214.26 | 77.77 | 0.23 | 111.43 | 9.71 | 2.47 |
| **6c** | 215.05 | 17.04 | 87.47 | <2.5 | 2.46 | 1066.84 | 262.24 | 0.20 | 89.85 | 6.81 | 2.39 |
| **6d** | 732.33 | 0 | 106.17 | 13.36 | 6.90 | 73.23 | <10 | 10 | 71.25 | 7.59 | 10.28 |
| **6e** | 252.48 | 10.05 | 73.23 | <3.4 | 3.45 | 824.49 | 50.29 | 0.31 | 76.34 | 4.04 | 3.31 |
| **6f** | 318.45 | 32.37 | 148.80 | 21.75 | 2.14 | 354.49 | 108.67 | 0.90 | 82.82 | 6.77 | 3.84 |
| **7a** | 965.51 | 16.90 | 112.23 | <8.6 | 8.60 | 112.23 | <7.6 | 8.60 | 105.86 | 4.81 | 9.12 |
| **7b** | 851.70 | 100.61 | 112.23 | <7.6 | 7.59 | 112.23 | <7.6 | 7.59 | 114.79 | 10.15 | 7.42 |
| **7c** | 458.63 | 82.72 | 112.23 | <4.1 | 4.09 | 172.49 | 17.52 | 2.66 | 91.33 | 2.93 | 5.02 |
| **7d** | 1019.36 | 0 | 101.94 | <10 | 10 | 101.94 | <10 | 10 | 106.65 | 16.58 | 9.56 |
| **7e** | 81.93 | 22.41 | 196.96 | 80.93 | 0.42 | 56.62 | 4.55 | 1.45 | 107.08 | 17.19 | 0.77 |
| **7f** | 636.48 | 5.64 | 214.08 | 33.80 | 2.97 | 87.32 | 9.53 | 7.29 | 156.74 | 21.63 | 4.06 |
| **7g** | 940.51 | 0 | 94.05 | <10 | 10 | 94.05 | <10 | 10 | 230.13 | 25.12 | 4.09 |
| **11a** | 59.12 | 6.89 | 35.55 | 3.98 | 1.66 | 402.19 | 87.55 | 0.15 | 140.25 | 14.72 | 0.42 |
| **11b** | 460.34 | 16.46 | 62.41 | <7.4 | 7.38 | 32.02 | 0 | 14.38 | 53.67 | 3.49 | 8.58 |
| **11c** | 27.88 | 3.12 | 92.72 | 9.12 | 0.30 | 248.85 | 59.05 | 0.11 | 69.93 | 2.96 | 0.40 |
| **14a** | 83.61 | 8.47 | 289.36 | 72.21 | 0.29 | 228.61 | 17.48 | 0.37 | 71.16 | 6.47 | 1.18 |
| **14b** | 627.41 | 0 | 63.59 | 7.66 | 9.87 | 62.74 | <10 | 10 | 50.60 | 2.34 | 12.40 |
| **14c** | 20.81 | 0.23 | 18.17 | 1.80 | 1.11 | 128.56 | 18.17 | 0.16 | 46.66 | 3.59 | 0.43 |
| **14d** | 5.91 | 0.32 | 3.96 | 0.20 | 1.49 | – | – | – | 33.88 | 3.01 | 0.15 |
| **17a** | 729.15 | 0 | 72.92 | <10 | 10 | 72.92 | <10 | 10 | 70.19 | 8.98 | 10.39 |
| **17b** | 12.70 | 2.58 | 16.50 | 1.92 | 0.77 | 115.72 | 73.34 | 0.11 | 99.31 | 4.90 | 0.13 |
| **21a** | 83.61 | 8.47 | 289.36 | 72.21 | 0.29 | 228.61 | 17.48 | 0.37 | 71.16 | 6.47 | 1.18 |
| **21b** | 49.16 | 9.44 | 102.40 | 2.70 | 0.48 | 152.04 | 19.52 | 0.32 | 98.12 | 9.62 | 0.50 |
| **21c** | 23.20 | 3.45 | 9.30 | 0.61 | 2.49 | 24.33 | 9.03 | 0.95 | 71.41 | 10.21 | 0.32 |
| **21d** | 276.03 | 4.56 | 691.27 | 137.29 | 0.40 | 259.93 | 110.61 | 1.06 | 75.37 | 4.89 | 3.66 |
| **21e** | 254.35 | 13.34 | 73.99 | <3.4 | 3.44 | 734.71 | 424.19 | 0.35 | 61.40 | 5.93 | 4.14 |

is not involved in the redox cycle of the enzyme and that the core is unique in this class of compounds.

The experimental data presented herein provided more accurate bioinformatics simulations as computational tools were used to recreate the allosteric pocket of the molecules through two different types of molecular docking for determining the best

**Table 2**
Pivotal amino acids and interaction distance related to bioactivity.

| | 14-b | 14-c | 17-a | 17-b | 21-c | R1 | R5 |
|---|---|---|---|---|---|---|---|
| **Ser-14** | x | x | x | x | x | 3,4 HB | X |
| **Leu-17** | 4,0 PS | 4,9 PS | 4,8 PS | 4,5 PS | 4,8 PS | 3,6 HB | X |
| **Trp-21** | x | 5,6 PS | x | X | 5,2 PS | 3,5 HB | 4,3 PS |
| **Ser-109** | 3,0 HB | x | 2,8 HB | 2,8 HB | 3,0 HB | 2,9 HB | X |
| **Tyr-110** | 3,7 HB | 2,9 HB | 4,1 PS | 4,1 PS | 5,3 PS | 3,1 HB | 2,7 HB |
| **Met-113** | 4,3 PS | 4,8 PS | 4,3 PS | 4,3 PS | 4,7 PS | 5,1 PS | 4,8 PS |
| **Antileishmanial activity (μM)** | 63,6 | 18,2 | 72,9 | 16,5 | 9,30 | 3,0 | 132,8 |
| **Affinity (Kcal/mol)** | −6,9 | −7,2 | −6,6 | −6,6 | −8,0 | −7,0 | −5,5 |

*HB: Hydrogen bond.
** PS: Pi-stacked.
*** Distance expressed in Å

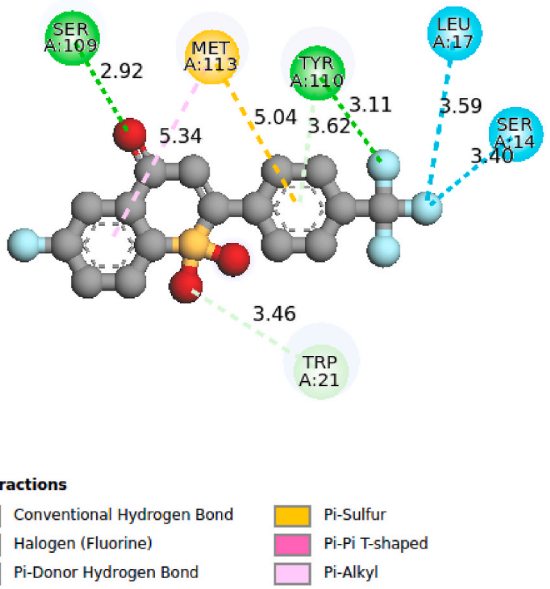


**Fig. 10.** Interhelical disruption simulated by interaction between R1 and TR.

enzyme–ligand model fit.

## Author contribution statement

Cristian Ortiz Bonilla: Conceived and designed the experiments; Performed the experiments; Analyzed and interpreted the data; Wrote the paper.

Matthias Breuning: Analyzed and interpreted the data; Wrote the paper.

Sara Robledo; Fernando Echeverri; Wiston Quiñones: Contributed reagents, materials, analysis tools or data.

Esteban Vargas: Conceived and designed the experiments; Analyzed and interpreted the data; Contributed reagents, materials, analysis tools or data; Wrote the paper.

## Data availability statement

Data included in article/supp. material/referenced in article.

## Declaration of competing interest

The authors declare that they have no known competing financial interests or personal relationships that could have appeared to influence the work reported in this paper

## Acknowledgements

The authors would like to thank Universidad de Antioquia, Colombia (CODI) for funding the project "2020-33772-Preparación de nuevos agentes antimaláricos."

## Appendix A. Supplementary data

Supplementary data to this article can be found online at https://doi.org/10.1016/j.heliyon.2023.e17801.

## References

[1] World Health Organization, Neglected Tropical Diseases [Internet] [cited 2023 Jun 11]. Available from:, 2023 https://www.who.int/teams/control-of-neglected-tropical-diseases/overview.
[2] Divakar Goli, Saurabh Bhatia, Leishmaniasis : Biology, Control and New Approaches for its Treatment, vol. 1, Taylor & Francis Group, 2017, pp. 88–95.
[3] A.J. Schvartzapel, L. Zhong, R. Docampo, J.B. Rodriguez, E.G. Gros, Design, Synthesis, and Biological Evaluation of New Growth Inhibitors of Trypanosoma cruzi (Epimastigotes), 1997.
[4] I. Ahmad, V. Pathak, P.G. Vasudev, H.K. Maurya, A. Gupta, Borontribromide-mediated C-C bond formation in cyclic ketones: a transition metal free approach, RSC Adv. 4 (47) (2014) 24619–24634.
[5] N. Sharma, A.K. Shukla, M. Das, V.K. Dubey, Evaluation of plumbagin and its derivative as potential modulators of redox thiol metabolism of Leishmania parasite, Parasitol. Res. 110 (1) (2012) 341–348.
[6] H. Bauer, K. Fritz-Wolf, A. Winzer, S. Kühner, S. Little, V. Yardley, et al., A fluoro analogue of the menadione derivative 6-[2′-(3′-methyl) -1′,4′-naphthoquinolyl] hexanoic acid is a suicide substrate of glutathione reductase. Crystal structure of the alkylated human enzyme, J. Am. Chem. Soc. 128 (33) (2006) 10784–10794.
[7] M. Omar, F. Khan, Trypanothione reductase: a viable chemotherapeutic target for antitrypanosomal and antileishmanial drug design, Drug Target Insights [Internet] 2 (2007) 129–146. Available from: www.dndi.org.
[8] M. Boiani, L. Piacenza, P. Hernández, L. Boiani, H. Cerecetto, M. González, et al., Mode of action of Nifurtimox and N-oxide-containing heterocycles against Trypanosoma cruzi: is oxidative stress involved? Biochem. Pharmacol. 79 (12) (2010) 1736–1745.
[9] E. Vargas, F. Echeverri, I.D. Vélez, S.M. Robledo, W. Quiñones, Synthesis and evaluation of thiochroman-4-one derivatives as potential leishmanicidal agents, Molecules 22 (12) (2017).
[10] Y.A. Upegui Zapata, F. Echeverri, W. Quiñones, F. Torres, M. Nacher, L.I. Rivas, et al., Mode of action of a formulation containing hydrazones and saponins against leishmania spp. Role in mitochondria, proteases and reinfection process, Int. J. Parasitol. Drugs Drug Resist. 13 (2020) 94–106.
[11] P. Baiocco, G. Poce, S. Alfonso, M. Cocozza, G.C. Porretta, G. Colotti, et al., Inhibition of Leishmania infantum trypanothione reductase by azole-based compounds: a comparative analysis with its physiological substrate by x-ray crystallography, ChemMedChem 8 (7) (2013) 1175–1183.
[12] P.A. Denis, Basis set requirements for sulfur compounds in density functional theory: a comparison between correlation-consistent, polarized-consistent, and Pople-type basis sets, J. Chem. Theor. Comput. 1 (5) (2005) 900–907.
[13] J. Eberhardt, D. Santos-Martins, A.F. Tillack, S. Forli, AutoDock vina 1.2.0: new docking methods, expanded force field, and Python bindings, J. Chem. Inf. Model. 61 (8) (2021) 3891–3898.
[14] O. Trott, A.J. Olson, AutoDock Vina: improving the speed and accuracy of docking with a new scoring function, efficient optimization, and multithreading, J. Comput. Chem. 31 (2) (2010) 455–461.
[15] A. Grosdidier, V. Zoete, O. Michielin, SwissDock, a protein-small molecule docking web service based on EADock DSS, Nucleic Acids Res. 39 (SUPPL. 2) (2011).
[16] A. Grosdidier, V. Zoete, O. Michielin, Fast docking using the CHARMM force field with EADock DSS, J. Comput. Chem. 32 (10) (2011) 2149–2159.
[17] F.F. Fleming, L. Yao, P.C. Ravikumar, L. Funk, B.C. Shook, Nitrile-containing pharmaceuticals: efficacious roles of the nitrile pharmacophore, J. Med. Chem. 53 (2010) 7902–7917.
[18] S.A. Pulido, D.L. Muñoz, A.M. Restrepo, C.V. Mesa, J.F. Alzate, I.D. Velez, et al., Improvement of the green fluorescent protein reporter system in Leishmania spp. for the in vitro and in vivo screening of antileishmanial drugs, Acta Trop. 122 (1) (2012) 36–45.
[19] F.S. Buckner, C.L.M.J. Verlinde, AC La Flamme, W.C. Van Voorhis, Efficient technique for screening drugs for activity against trypanosoma cruzi using parasites expressing-galactosidase, Antimicrob. Agents Chemother. 40 (11) (1996) 2592–2597. Available from: https://journals.asm.org/doi/10.1128/AAC.40.11.2592?url_ver=Z39.88-2003&rfr_id=ori:rid:crossref.org&rfr_dat=cr_pub%20%200pubmed.
[20] S. Nkhoma, M. Molyneux, S. Ward, In Vitro Antimalarial Susceptibility Profile and PRCRT/PFMDR-1 Genotypes of Plasmodium Falciparum Field Isolates from Malawi, 2007.
[21] F. Mohammed, M. Gorla, V. Bisoyi, P. Tammineni, N.B.V. Sepuri, Rotenone-induced reactive oxygen species signal the recruitment of STAT3 to mitochondria, FEBS Lett. 594 (9) (2020 May 1) 1403–1412.
[22] J.F. Honek, in: N.D. Rawlings, G. Salvesen (Eds.), Chapter 181 - Aeruginolysin, third ed.Handbook of Proteolytic Enzymes [Internet], Academic Press, 2013, pp. 867–872. Available from: https://www.sciencedirect.com/science/article/pii/B9780123822192001812.
[23] C. Ortiz, F. Echeverri, S. Robledo, D. Lanari, M. Curini, W. Quiñones, et al., Synthesis and evaluation of antileishmanial and cytotoxic activity of benzothiopyrane derivatives, Molecules 25 (4) (2020).